CATÓLICA

UNIVERSIDADE CATÓLICA PORTUGUESA | PORTO

Escola Superior de Biotecnologia

The Effect of Sonication on Electrospun Silk Fibroin/ PEO Membranes for Periodontal Regeneration

by

Ricardo Lopes de Almeida Guimarães Serôdio

March 2017

The Effect of Sonication on Electrospun Silk Fibroin/ PEO Membranes for Periodontal Regeneration

Thesis presented to *Escola Superior de Biotecnologia* of the *Universidade Católica Portuguesa* to fulfill the requirements of Master of Science degree in Biomedical Engineering

by

Ricardo Lopes de Almeida Guimarães Serôdio

Radboud University Medical Center, Radboud University Nijmegen, Comeniuslaan 4, 6525 HP Nijmegen, Holanda

Escola Superior de Biotecnologia, Universidade Católica Portuguesa, Rua. Arq Lobão Vital, Apartado 2511, 4201-401 Porto, Portugal

Supervised by

Prof. Fang Yang; Prof. Ana Leite Oliveira; Sónia De Lacerda Schickert

March 2017

Resumo

A periodontite é uma das patologias orais mais comuns, que envolve a destruição da estrutura de suporte do dente, sendo responsável pela degradação e perda das estruturas periodontais. A Regeneração Guiada de Tecidos (RGT) tem vindo a ganhar reconhecimento na tentativa de restaurar o tecido periodontal perdido e promovendo a integração tecidular, incluindo a formação de novo ligamento periodontal funcionalmente orientado para o cimento e o osso alveolar.

Recentemente, grandes avanços têm vindo a ser feitos na área da RGT, usando materiais e técnicas de processamento inovadoras. No entanto, na maioria das vezes, os requisitos físico-químicos, biológicos e mecânicos não são totalmente cumpridos, o que limita a sua aplicação clínica. A fibroína de seda (SF) foi recentemente reconhecida como um material de elevado potencial para várias aplicações biomédicas, incluindo a regeneração de tecidos. Tendo em conta de que se trata de uma proteína estrutural, naturalmente fiada por insectos, a SF surge assim como um material ideal a ser processado por tecnologia de electrospinning, visando o tratamento periodontal. O princípio básico por detrás desta técnica é a aplicação de uma alta tensão sobre uma solução polimérica que é expelida a partir de uma agulha formando nanofibras que se irão depositar sob a forma de uma matriz polimérica. Um dos parâmetros mais importantes para atingir as condições ótimas de processamento e a qualidade da fibra é a viscosidade da solução.

Assim, com este estudo procurou-se investigar a possibilidade de utilizar um tratamento de ultra-sonicação antes do electrospinning como estratégia para melhorar fisicamente as propriedades reológicas de soluções de SF/óxido de polietileno (PEO) a diferentes concentrações (10 %, 20 % e 30 % de PEO (w/v)), para melhorar a processabilidade das nanofibras.

A influência do tempo de sonicação (0, 7,5, 15 e 20 minutos) nas propriedades da solução foi estudado. Os ensaios reológicos demonstraram que o tratamento de ultra-sonicação melhorou a viscosidade das soluções SF/PEO. As membranas produzidas apresentaram maior diâmetro de fibra após sonicação e propriedades mecânicas melhoradas em condições secas e húmidas. Por espectroscopia de infravermelho demonstrou-se que, embora as membranas SF tivessem sofrido algumas transições conformacionais com o aumento do tempo de sonicação, no sentido da formação de estruturas em folha beta, a sua estrutura é maioritariamente composta por conformação amorfa. Adicionalmente foram realizados ensaios de permeabilidade, que demostraram que a taxa de transmissão de vapor de água é elevada, permitindo a difusão dos nutrientes enquanto atua como uma barreira celular. Finalmente, ensaios preliminares de cultura de células in vitro utilizando células primárias do ligamento periodontal (PDLs) indicam que as membranas desenvolvidas suportaram a adesão celular e a proliferação indicando boa viabilidade celular como revelado pelos resultados de ADN. O presente trabalho constitui um progresso para o processamento de membranas de SF spinnadas viáveis para a regeneração periodontal, uma vez que demonstra que é possível ajustar a viscosidade das soluções de SF para obter condições de processamento óptimas utilizando um simples passo de sonicação antes do processo electrospinning , minimizando a quantidade de polímero sintético a ser utilizado.

Abstract

Periodontal disease is one of the most common oral diseases involving destruction of the tooth-supporting apparatus and is responsible for the decay and loss of the periodontal structures in adults. Guided Tissue Regeneration (GTR) has recently gained recognition in the attempt to restore the lost periodontal tissues, promoting tissue integration, including the formation of new periodontal ligament functionally oriented to the newly formed cementum and alveolar bone.

Recently, major advancements have been done in the development of membrane systems for the guided tissue regeneration (GTR) technique using innovative materials and processing techniques. However, most of them still do not fulfill all the physicochemical, biological and mechanical requirements, limiting their clinical application. Silk Fibroin (SF) has been recently recognized as a high potential material for several biomedical applications, including tissue regeneration. Taking into account that it is a structural protein, already spun by insects in nature, SF emerges as a prospective material to be processed by electrospinning, aiming at periodontal treatment. The basic principle behind this technique is the application of a high voltage over a polymeric solution suspended from a needle generating polymer nanofibers that will deposit under the form of a nonwoven mat. Amongst the most important parameters to achieve optimal processing conditions and fiber quality is the viscosity of the starting solution.

This study investigates the possibility of combining a sonication treatment prior to electrospinning as a strategy to physically enhance the rheological properties of SF/poly (ethylene oxide) (PEO) solutions of different concentrations (10 %, 20 % and 30 % PEO (w/v)), and therefore to improve the spinability of the system.

The influence of sonication time (0, 7.5, 15, and 20 minutes) on the solution properties was studied. The rheological tests indicated that sonication improved the viscosity of SF/PEO solutions. The electrospun SF/PEO membranes from the sonicated solutions demonstrated higher fiber diameter and improved mechanical properties in dry and wet conditions.

Infrared spectroscopy, demonstrated that, although the SF membranes had undergone some conformational transitions with the increasing of sonication time, their structure was mainly composed by amorphous conformation. Permeability assays were also used as a complementary test, showing that the water vapor transmission range is high allowing for the diffusion of the nutrients while acting as a cell barrier. Finally, preliminary *in vitro* cell culture assays using primary cells from the periodontal ligament (PDLs) indicated that the developed membranes supported cell adhesion and proliferation indicating good cell viability as revealed by the DNA results. The present developed work constitutes a step forward towards the processing of viable electrospun SF-based membranes for periodontal regeneration since it demonstrates that it is possible to tune the viscosity of SF solutions to achieve optimal processing conditions using a simple sonication step prior to the electrospinning process, minimizing the amount of synthetic polymer to be used.

Acknowledgments

This Master's dissertation represents an important milestone in my life, an end of a cycle during which I grew up personally and professionally. The Catholic University of Portugal, particularly the Faculty of Biotechnology, represents by excellence the most determining and exciting period of my life. This dissertation is the culmination of a course, which could only be achieved due in large part to the contribution and encouragement of several people.

Foremost, I would like to express my deep gratitude to Prof. Draª Ana Leite Oliveira, who guided me through this wonderful journey. For the invaluable support, personal generosity, knowledge sharing, opinions and constructive criticism, but especially for the words of encouragement and for always pushing me further. I could not imagine having a better mentor for my dissertation than the one I had.

My sincere gratitude also goes to Drª Fang Yang for offering me the opportunity of working and be part of the Tandheelkunde Radboudumc research group. For the wisdom, total support, guidance, and availability in helping me with problems and doubts that have arisen throughout my work. Her guidance and enthusiasm made this experience gratifying.

I would also like to thanks to Sónia De Lacerda Schickert for her motivational support, massive patience and resolute enthusiasm that kept me constantly engaged with my research. For her kindness and hospitality since the first day. Her unconditional care made not only this project achievable but also made me grow as professional and as person.

I thank my fellow labmates and all the Tandheelkunde family for having welcomed me with open arms, and for the powerful and gratifying experiences that helped make my time in Nijmegen rewarding. And I also thank to my co-workers in the Faculty of Biotechnology for helping me with the research.

To Alessandra Curci and Mariateresa Brindisi for their friendship, for caring, for their fiery Italian temperaments, for the endless karaoke and dance sessions, for the gastronomic experiences, for their laughs and for giving me so many special memories. Despite the distance, they will always be in my heart.

To Tomás Marques, my good old friend and roommate with who I shared this experience. For your fellowship and support at all times. To him, I owe all the awesome stories I can tell today.

To my friends Bryan Pereira, Filipa Costa, Filipe Coutinho, Francisco Garrett, João Alves, Ricardo Queiroz, Susana Hawkins and Tiago Abreu for always believing in me, and giving me the extra push I needed.

Lastly, a special thanks to my parents and sisters that encouraged and supported throughout this journey. For their unconditional love and concern that made me who I am today. To them I dedicate this work.

Contents

List of figures

List of tables

List of abbreviations

PDL	Periodontal ligament
GTR	Guided Tissue Regeneration
ECM	Extracellular matrix
MSC	Mesenchymal stem cells
PTFE	Polytetrafluoroethylene
e-PTFE	expanded polytetrafluoroethylene
d-PTFE	high – density polytetrafluoroethylene
Ti	Titanium
LiBr	Lithium bromide
PEO	Polyethylene oxide
Non-son	Non sonicated
SEM	Scanning electron microscopy
FTIR	Fourier Transform Infrared
UTS	Ultimate tensile strength
DNA	Deoxyribonucleic acid

I. Introduction

1.1 The periodontal structure

The periodontium is the supporting structure (Figure 1) responsible for the attachment of the teeth to the surrounding tissues. Besides playing an important role in the mechanical and chemical preservation of the tooth, this structure also performs an active role in the protection against microorganisms. It can be divided into two main regions: the mineralized part, composed of alveolar bone and root cementum and a non-mineralized part that includes the periodontal ligament and the gingiva.[1,2]

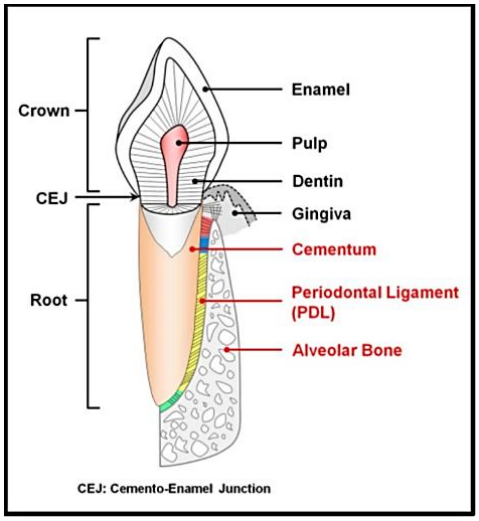

Figure 1- Anatomical illustration of the periodontal tissue structure[1]

The mineralized part of the periodontal structure includes the alveolar bone, a bony structure of the maxilla/ mandible that forms the tooth sockets, and the root cementum, a specialized connective tissue that surrounds the root of the teeth.[1,3] These structures provide support and protection for the roots of the teeth. The alveolar bone contains a region of compact bone (called the lamina dura) which is attached to the cementum of the roots by the periodontal ligament.[3,4] The root cementum is composed by two distinct parts: an acellular and a cellular cementum. The acellular cementum is present majorly in the coronal half of the root. The cellular cementum, on the other hand, can be found more frequently on the apical half, and is mainly composed by collagen fibers and cementocytes.[3]

The non-mineralized structure comprises the gingiva, a soft tissue part of the oral mucosa that lies over the maxilla and mandible inside the mouth. This structure provides a tissue seal around the teeth by covering their cervical portions and the alveolar bone of the jaws. The gingiva can be divided into two main parts: the marginal or free gingiva and the attached gingiva (Figure 2).

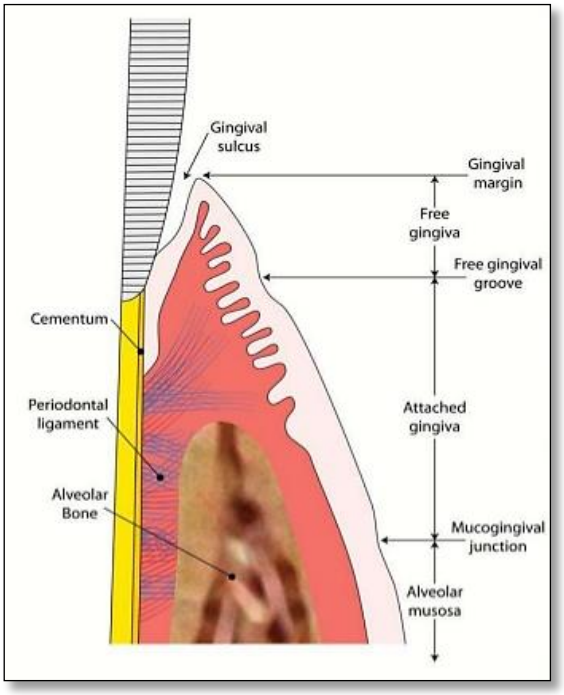

Figure 2 - Anatomy of the gingiva.[5]

The marginal gingiva is the terminal border of the gingiva surrounding the teeth and it is demarcated from the attached gingiva by a shallow depression, the free gingival groove. This gingival groove is located at the base of the gingival sulcus and it is positioned at the cemento-enamel junction (CEJ; Figure 1) level. A deep depression (depth > 3mm) is usually an indication of an unhealthy periodontium.[6]

Firmly connected to the periosteum (connective tissue cover) of the alveolar bone and to the roots cementum, we have the attached gingiva, a continuity to the marginal gingiva. This structure is demarked by the mucogingival junction (MJC) and by the gingival groove in the apical and coronal direction respectively.[3] In addition to preventing the marginal gingiva to be pulled away from the tooth when tension is applied to the alveolar mucosa it also allows the gingiva to withstand mechanical forces.

Besides the gingiva, the non-mineralized unit also embraces the periodontal ligament (PDL). PDL is a soft connective tissue located between the cementum that surrounds the root of the tooth and connects it to the alveolar bone of the tooth socket.[3,7]

Collagen is the most important component of the PDL. Despite having already been reported the presence of collagen type IV, V, VI and XII,[3,6] the extracellular compartment of PDL is mainly composed of type I and type III collagen, in the form of bonded fibers.

This bundle of collagenous fibers (Figure 3) can be arranged in six groups: alveolar crest fibers, horizontal fibers, oblique fibers, apical fibers, interradicular fibers and Sharpey's fibers. Playing an important role in anchorage and maintenance of PDL space. Besides collagen, other major proteins are present in the PDL, like glycoproteins[3,6,7], proteoglycans[3,6,7], growth factors[2,3,7], enzymes[3,7] and cytokines.[2,3,7]

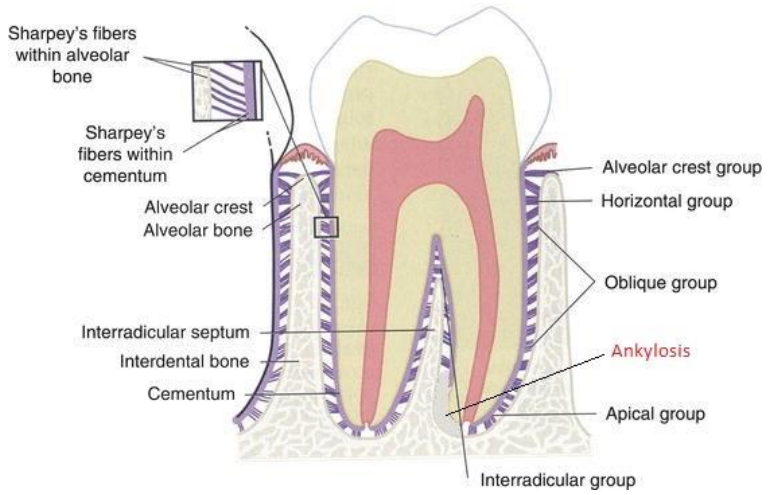

Figure 3 - Periodontal ligament fibers.[129]

The PDL serves primarily a supportive function by attaching the tooth to the surrounding alveolar bone. Also serving as a shock- absorber to the impact of the mastication occlusal forces. The applied load on the PDL is dissipated to the alveolar bone trough the PDL fibers, blood vessels and extravascular tissue fluid. Furthermore, PDL also have a proprioception function that allows the organism to feel the tooth and detect pressure and pain. This function is ensured by a large blood vessels network, sensory nerve fibers and by the presence cells associated with neurovascular elements in the surface of PDL.

A nutritive function is also guaranteed by the major blood supply originating from the dental arteries. Thus, providing nutrients to the cementum and bone.

Finally, PDL also provides cells to participate in the formation and remodeling of cementum and bone. Undifferentiated mesenchymal cells, can differentiate into cells that form bone (osteoblasts), cementum (cementoblasts) and connective tissue fibers (fibroblasts).[3]

In addition, the surface of PDL also includes other cellular elements. Epithelial rest cells of Malassez close to the apical area of the cementum and immune system cells as neutrophils, lymphocytes and macrophages.

1.2 Periodontal inflammatory disease

Periodontal disease is one of the most common oral diseases and it is responsible for the decay and loss of the periodontal structures in adults.[8] The development of these diseases is usually associated with the accumulation of an organized bacterial biofilm near the tooth also known by dental plaque.

This dental biofilm usually arises due to the aqueous environment present in the oral cavity, suitable for the growth and proliferation of bacterial communities.[9,10]

The bacterial products, such as lipopolysaccharide (LPS), deposit and calcify to form tartar or calculus.[1,10] These metabolic products, stimulate chemical inflammatory mediators[8], like cytokines, to signal precursor cells to differentiate and activate osteoclastic cells and proteinases[8], which will degrade the tooth surface and the adjacent periodontal tissues, thus initiating an inflammatory response as the body tries to fight the infection.[8]

This immuno-inflammatory response usually emerges in the gingival tissues, leading to development of gingivitis. Gingivitis is a non-destructive and reversible periodontal disease, characterized by the inflammation of the gingiva.[8,11] Redness, swelling and gingival bleeding are the primarily signs of gingivitis development.[8]

However, if the plaque is not properly removed, the bacterial microflora starts to invade deeper tissues causing the deterioration of the collagen and consequently the periodontal ligaments that give support to the teeth.[1,12] As a result, a phenomena known as “periodontal pocket”[12] occur. Due to the resorption of the alveolar bone and the relocation of the gingiva along the tooth surface.

As this hollow between the tooth and gum grows, the bacterial microflora can easily settle and start to obtain nutrients from the surrounding periodontal tissues. Besides that, with the increase of the biofilm thickness, nutrients and oxygen diffusion from the tissues through the biofilm matrix becomes gradually more difficult.[10]

With the progression of this condition, it is noteworthy the shift of microflora type involved. As the gram-positive aerobic species of microorganisms in healthy individuals give way to gram-negative anaerobic species[10] (as *Phorpyromonas gingivalis, Aggregatibacter actynomicetemcomitans, Prevotella intermedia, Fusobacterium nucleatum, Eikenella corrodens, Treponema denticola, Campylobacter rectus, Capnocytophaga, Tannerella forsythia*) in unhealthy patients.[12] As a result, gingivitis progress to a more severe periodontal condition (Figure 4), periodontitis.

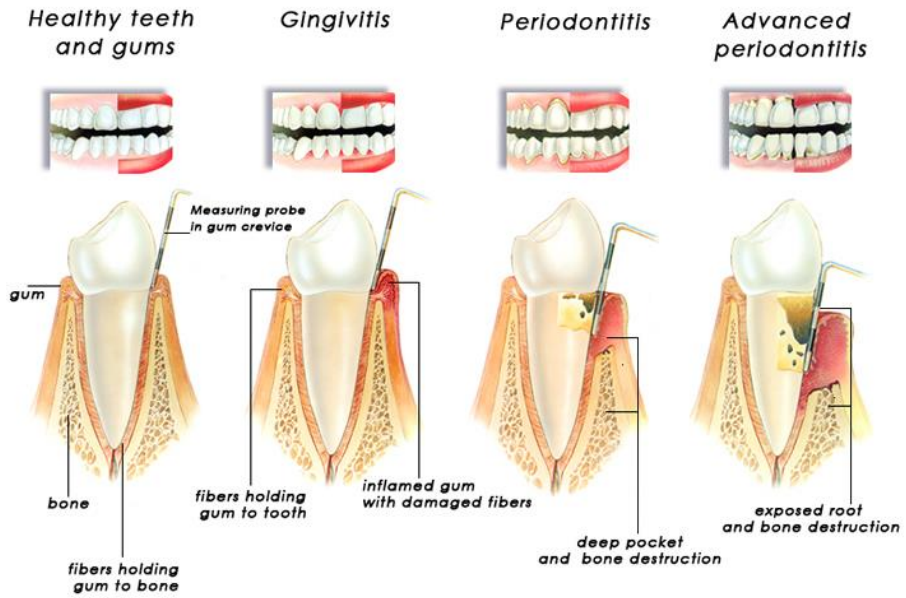

Figure 4 - Progression of gum disease.[130]

Periodontitis is a chronic infection involving destruction of tooth-supporting apparatus.[3,8]

It can be classified into chronic periodontitis (the most common form), when we face a slow evolution of this condition, or into aggressive periodontitis, a more severe and advanced form that affects between 10-15% of the world population[12–14]. This last, is characterized by the progression of periodontal tissue destruction, destruction of the PDL, deepening of the periodontal pockets (Figure 4) and subsequently the loss of a support structure of the teeth. [12]

There are several risk factors that can trigger the onset of a periodontitis condition. Poor oral hygiene, smoking, non-controlled diabetes, obesity, low dietary of calcium and vitamin D, osteoporosis and stress are the most common.[8,9,12,15] Gender and genetics (inheritance) can also have an important role on the increasing incidence of the disease on the population. Genetic susceptible individuals may present a disorder on its genotype, causing a disproportion in the anti-inflammatory and inflammatory mediators. The over expression of pro-inflammatory mediators and enzymes and the lack of protective anti-inflammatory mediators promotes an inflammatory response that leads to the destruction of the periodontium.[8]The activation and deactivation of these mediators will be studied further on.

Identification of these risk factors as well as the patient medical and dental history can help to prevent and determine a suitable treatment.[8,9]

A “National Health and Nutrition Examination Survey” study carried in the United States, estimated that between 2009 and 2010, 47.2% or 64.7 million adults aged 30 and over suffered from periodontitis. This number increases up to 70.1% in adults with 65 or older”.[4]

Once the lesions caused by this condition are so advanced that the tissues cannot heal by themselves, medical intervention and treatment becomes inevitable.

1.3 Prevention and treatment of Periodontitis

In the past, due to the lack of knowledge of the host response to treatments, periodontal maintenance focused only on the reduction of the microbial load.[8]

Nowadays, a variety of non-surgical and surgical approaches emerged to achieve surgical pocket reduction, to increase the attachment and help the regeneration of the periodontium tissues.[8] By complementing different surgical strategies with the reduction of microbial flora, the chances of clinical success improves.

Non-surgical therapy aims to diminish tissue inflammation and eliminate microbial biofilm.[16] Scaling and root-planning are two types of non-surgical deep cleaning treatments that are strategically combined to remove dental plaque and the bacterial microflora that is gathered along the tooth root.[11] This type of treatments allows to control the periodontal disease, but does not restore periodontal health. The systemic or local administration of antimicrobial agents or antibiotics has been also studied[8,16,17] as a complement to mechanical treatment. However, antibiotics are not innocuous dugs, and therefore should only be used when the patient condition does not respond to the conventional treatment.[17]

Thus, to assure a long term maintenance of the periodontal apparatus, surgical treatment is advisable.

Surgical procedures can be required to guarantee the regeneration of the tooth- supportive structures and to restore periodontal functions.

Flap surgery is probably the most conservative and versatile technique used nowadays for gum diseases treatment.[18] This procedure consists of making an internal opening in which the gums are separated from the teeth and then folded back (gingival flap) temporarily. This allows the periodontist to reach the root of the tooth, remove the inflamed tissue and repair the periodontal tissue complex.[3,18] Non-surgical methods can also be applied for a deeper clean.

Still, this technique takes on some post-operation risks. Bleeding and swelling, infection, recession of the gums on the treated area, increased sensitivity and propensity to develop cavities on the roots.[3]

In addition to flap surgery, bone and tissue replacement grafts[19], plastic surgery for gingival augmentation[3,20,21] and occlusal adjustment[3,22] can also be used to facilitate orthodontic treatment.

For the most severe cases of periodontitis, when tooth loss occurs, dental implants or dentures made of synthetic materials are inevitable. [1] Nevertheless, most of the materials used to replace the teeth have a limited lifetime, partially replacing the mechanical function of teeth and poorly promoting osteointegration.[23] The use of bioactive molecules, stem cell therapies and biomaterial fillings can be used to improve the bone-implant anchorage and symbioses.[12]

When the loss of the periodontium structure is at an advanced stage, guided tissue regeneration (GTR) technique, can be used to stimulate the regeneration of the periodontal tissues.

This technique, which will be discussed in the next chapter in further detail, relies on several procedures that attempt to regenerate damaged periodontal structures through differential tissue responses (resorting or not to bone grafts).[1,3,16,24,25]

Since each case is different, it is not possible to predict with certainty which kind of treatment will be successful in the long-term. However the most appropriate treatment should be selected according to the developmental stage of the disease.

1.4 Repair and regeneration of periodontal tissues

Regenerative periodontal therapy comprises techniques specially designed to fully restore the architecture and function of the affected area. However, must often only tissue repair is achieved.[26]

Thereby, other surgical approaches begun to gain recognition in the attempt to restore the lost periodontal tissues,[26] promoting tissue integration, including formation of new periodontal ligament with its collagen fibers functionally oriented to the newly formed cementum and alveolar bone.[2,3]

Based on this idea, the concept of guided tissue regeneration (GTR) was developed.

The GTR technique relies on the use of an occlusive membrane interfacing with gingival connective tissue and a PDL tissue, thus promoting wound repopulation by PDL cells which are able to induce periodontal tissue regeneration. [26]

The surgical procedure involves the placement of a thin membrane over the periodontal defect under the gingival flap. As can be seen in Figure 5, this technique can be combined with flap surgery. In the end the flap is sutured over the membrane and therefore providing a support structure for the proliferation and differentiation of the PDL cells.

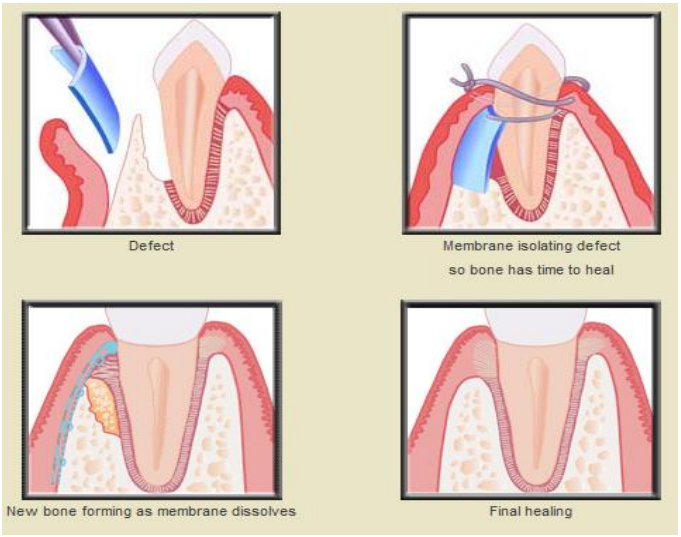

Figure 5 - GTR technique schematics.[131]

Thus, a tissue engineering approach for periodontal regeneration is advantageous. This will imply (Figure 6) the involvement of stem cells found within the periodontal tissues[6,14,27], which are isolated and induced to proliferate; a supporting structure[2,4,28] (membrane) that can act as a extracellular matrix (ECM), where the cells can be introduced to be subsequently implanted in the "*in vivo*" defect; and chemical mediators that stimulate and facilitate the tissue repair.[2,4,28]

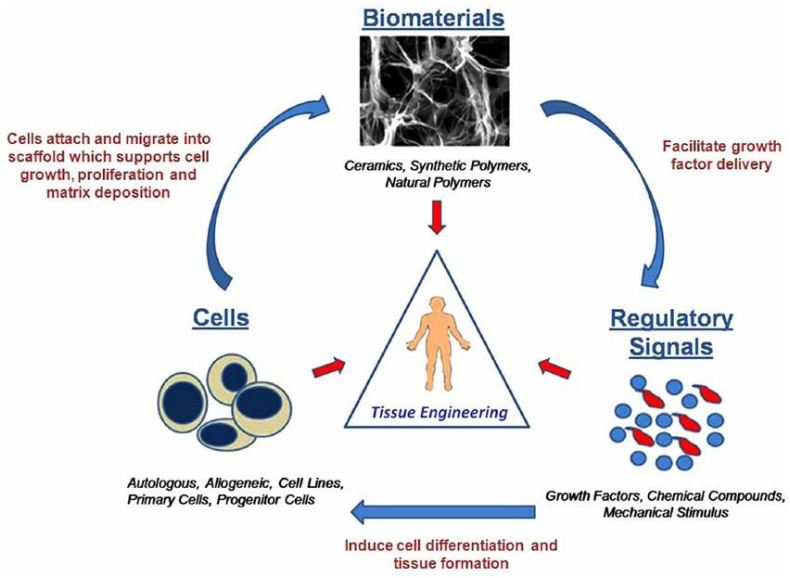

Figure 6 - Tissue engineering essential components.[132]

Neovascularization, i.e., formation of vessels is also a requirement to nourish the tissue to be formed. [2,28]

1.4.1 Cells and Signals

The recruitment of mesenchymal stem cells (MSC) plays an important role for the overall formation of a functional periodontium.[29] These cells are characterized by being undifferentiated, likely to renovate limitlessly, also capable to differentiate into a subpopulation of cells with very specific characteristics when subjected to certain physiological/experimental favorable conditions. [28]

This differentiation ability, can be proven by the several MSC cells subpopulation sources identified: dental pulp, exfoliated deciduous teeth, dental follicle, root apical papilla and PDL.[6,28]

The first stem cells were reported in the perivascular space of the PDL was in 1976 by Melcher.[4,21]

Later, Nyman (1982)[30], Gottlow (1984)[31] and Karring (1986)[32] proved that only PDL cells have the potential for regenerating the tooth apparatus.[30]

Years on, in 2004, PDL cells were for the first time isolated and studied for their response to stimuli, which identified similar properties to their progenitor cells, the MSCs.[14] The fibroblasts-like cells existing in the PDL are also able to express the transcription factor Runx2. A factor that is essential to promote the differentiation of adipocytes, osteoblasts-like cells and cementoblasts-like cells.[7,14]

Besides promoting the maintenance of the periodontium structure, the presence of collagen of type I, type III and fibronectin on the PDL fibroblast ECM contributes for the cell attachment to the nearby tissues.[2]

With the advance of studies in molecular and cell biology, the use of chemical mediators (growth factors) associated with PDL fibroblast began to gain importance in the promotion of periodontal regeneration.[14] Currently, platelet-derived growth factor (PDGF), insulin-like growth factor-I (IGF-I), transforming growth factor-β1 (TGF- β1) and fibroblast growth factors (FGF_S) are the most commonly signaling molecules used. This molecules, modulate cellular activity, by being directly/indirectly involved in the recruitment, proliferation, migration and differentiation of cells.[22,24,33,34] Which influences inflammatory and anti-inflammatory processes, wound healing, tissue regeneration, ECM formation and apoptosis and angiogenesis events. [12,21,22,24,27,34,35]

Still, further advances are necessary to correct problems associated with the application of growth factors. We highlight the rapid loss of the effect of the applied growth factors; the non-specific activity on different cellular lineages and the dependence of a high-dose application.

1.4.2 Supporting Structure

As has previously referred, a successful periodontal regeneration relies on the reconstruction of an epithelial seal, deposition of new acellular cementum and apposition of connective tissue fibers into the root surface, and restoration of the alveolar bone.[3]

The biological foundation of GTR is therefore based on the hypothesis that placing physical barriers at the wound site will prevent apical migration of the epithelium and gingival connective tissue cells of the flap,[25,29,36] thus providing space for the migration of PDL cells on the exposed root surface, which in turn will promote periodontal regeneration.[3,25]

The reconstruction of the periodontal structure requires a proper biomaterial, which can not only act as a temporary physical barrier but also be able to recruit and provide a niche repopulated with PDL cells.[4]

Currently, a wide diversity structures (carriers, grafts, scaffolds and membranes) have been described to be applied in periodontal defects to promote the regeneration of the periodontal tissue, including autogenous grafts[4], allogenic grafts[4], xenogeneic grafts[4] and natural components membranes[36–38] or synthetic carriers.[4,33]

Regardless of the used material, it is important to understand that certain parameters of these structures need to be secured, to assured to promote a bidirectional cell-membrane interaction.[4]

Apart from the biocompatibility requirements of the material with the surrounding structures of the periodontal ligament, the provided structure also needs to isolate the wounded space, [2,29,36,37,39] thus, excluding the invasion of undesirable cells.[25,29,36]

When compared to other therapeutic solutions like implants, prosthetics and biomaterials,[1] GTR membranes have shown the advantage of optimizing the re-growth of healthy tissue through a selective cell proliferation.[36,40] By physically prevent the contact between the gingival connective tissues and the root surface, only PDL-derived cells were allowed to repopulate the wounded area, allowing a faster and enhanced regeneration.[40]

Since space confinement is also critical, the adequate mechanical properties of the membrane need to be assured.[4] The barrier should be strong enough to avoid its own collapse and the collapsing of soft tissues nearby, when subjected to tissue tension in the flap/occlusion sites. Mechanically, the membrane should also be capable of reduce/eliminate the wound space. [21,29,33,36,41]

Besides that, the surface properties and chemical composition also play an important role on tissue integration by promoting cell adhesion, proliferation, migration and differentiation. [39,42] At last, the membrane must be able to easily adapt to the periodontal region and easy to manage clinically.[41] The degradation properties of a membrane should also be taken into consideration. Adequate degradation time matching the tissue regeneration rate of the periodontal tissue should be attained.

Given the potential of GTR membranes for tissue regeneration, new types of materials (natural and synthetic) as well as new processing strategies have been proposed in the latest years.

According to their degradation profile, GTR membranes can be designated as non-absorbable or absorbable.

1.4.3 Non-absorbable membranes

Non-absorbable membranes are able to preserve their structural integrity, when implanted in the host tissue.

The first membrane ever used on periodontal surgery, as a GTR product, was cellulose acetate laboratory filter paper by Nyman et al. in 1982.[29,36] Animal experiments were performed in order to study the regenerative potential of these membranes on the periodontium structures. The obtained results allow to observe the regeneration of the cementum, alveolar bone and periodontal tissues.

Nowadays, polytetrafluoroethylene (PTFE) membranes are well-recognized as a standard of non-absorbable membranes for clinical use. PTFE also known as Teflon is a biocompatible and inert polymer.[26,29,38] Its reduced reactivity, allow this material to have almost a nontoxic behavior to the biological tissues. Besides that, PTFE allows tissue ingrowth and avoids a host immune response after the implantation. [29,43]

When PTFE is subjected to high tensile stress it forms a compound with identical properties, the expanded polytetrafluoroethylene (e-PTFE). This component was the basis of the first approved non-absorbable membranes.[29,43]

However, several animal studies have proven that the exposure of the membrane to the oral cavity would bring some drawbacks to the regeneration process, due the high risk of infection.[43–45]

Further, after 4 to 6 weeks[43] a second surgical procedure is required for the removal of these membranes since they aren't biodegradable. This, adds the possibility of damaging the newly regenerated tissues, causing discomfort to the patient and the inherent costs of a second surgery.[3,29,37]

Besides e-PTFE, we can also include within the more common commercial non-absorbable membranes, high-density polytetrafluoroethylene (d-PTFE)[38,40,46] and titanium mesh[40,46] as presented in the Table 1.

Table 1 - Commercially available non-absorbable membranes for GTR.

Membranes	Commercial name	Manufacturer[40]	Materials	Properties
e-PTFE	Gore-Tex (Teflon)[47,48]	W. L. Gore & Associates, Inc.	e-PTFE[40,43,47,48]	Gold standard membrane for GTR[43]; Good space maintainer[38,40,47]; Good cell occlusion[47,48]; Stable structural integrity[47]; Easy handling[38,40]; Porosity : 0.5 -3µm[43,46]; Commercially discontinued[46]
	Gore-Tex-TI[38,40]	W. L. Gore & Associates, Inc.	Ti-e-PTFE[40]	Superior space maintainer[40]; Filler material unnecessary[40], Titanium must be shaped to allow space for tissue growth[38]
d-PTFE	High-density Gore-Tex[38,40]	W. L. Gore & Associates, Inc.	d-PTFE[38,40,46]	Porosity: 0.2- 0.3 µm[38,40]
	Cytoplast[40,43,46]	Osteogenics Biomedical.		Porosity: < 0.3 µm[40,43,46]; Anti-bacterial properties[43]
	TefGen FD[40,46]	Lifecore Bio-medical, Inc.		Porosity: 0.2- 0.3 µm[40,46]
	Nonresobable ACE[40,46]	Surgical supply, Inc.		Porosity: < 0.2 µm[40,46] Thickness: 0.2 µm[40,46]
Titanium mesh	Ti-Micromesh ACE[40,46]	Surgical supply, Inc.	Ti[40,46]	Porosity: 1,700 mm[40,46] Thickness: 0.1 mm[40,46]
	Tocksystem Mesh[40,46]	Tocksystem		Porosity: 0.1- 6.5 mm[40,46] Thickness: 0.1 mm[40,46]
	Frios BoneShields[40,46]	Dentsply Fria-dent		Porosity: 0.03 mm[40,46] Thickness: 0.1 mm[40,46]
	M-TAM[40,46]	-		Porosity: 1,700 mm[40,46] Thickness: 0.1 mm[40,46]

In order to exclude a second surgical procedure, the demand for absorbable biomaterials increased and bioabsorbable membranes began to be developed.[43]

1.4.4 Absorbable membranes

Despite sharing some properties with e-PTFE membranes (biocompatibility and desirable cell exclusion from the wounded space), absorbable membranes have been developed in order to bypass the complications of a second surgery.[43,49]

The list of materials used as a basis for the formulation of these membranes is wide. Polyglycolic acid (PGA)[38,40,43,46], polylactic acid (PLA)[38,40,43,46], polyglycolic acid copolymer (PLGA)[38,40] for the synthetic ones and natural periodontium tissues[47], chitosan[38,47], gelatin[38] and collagen[38,40,46] for the natural barriers, are just some of the most commonly used.[3,21,33,36,37] Some of them are shown in Table 2.

Table 2 - Commercially available absorbable membranes for GTR.

Membranes	Commercial name	Manufacturer	Materials	Properties
Natural and biodegradable (Collagen type I/III)	BioGide[38,40,43,46]	Osteohealth Company[40]	Porcine type I and III[38,40,43,46] / Bovine type I[43]	Resorption rate: 24 weeks[40,43,46] Mechanical strength: 7.5 MPa[40]
	BioMend[38,40,43,46]	Zimmer Biomet[38,40]	Bovine type I[38,40,46]	Resorption rate: 8 weeks[38,40,43,46] Mechanical strength: 3.2-22.5 MPa[40]
	BioMend Extend[38,43,48]	Zimmer Biomet[38]	Bovine type I[38]	Resorption rate: 18 weeks[38,43]
	Neomem[38,40,46]	Citagenix[38,40]	Bovine type I[38,40,46]	Resorption rate: 26-38 weeks[38,40,46]
	OsseoGuard[38,40,46]	BIOMET 3i[40]	Bovine type I[38,40,46]	Resorption rate: 24-32 weeks[38,40,46]
	Ossix[38,40,46,48]	OraPharma, Inc[40]/ Datum Dental Ltd[38]	Porcine type I[38,40,46]	Resorption rate: 16-24 weeks[38,40,46]
	TutoDent[38,48]	Tutogen Medical GmbH[38]	Bovine type I[38]	Resorption rate: 8-16weeks[38]
	Biosorb membrane[40,46]	3M ESPE[40]	Bovine type I[40,46]	Resorption rate: 26-38 weeks[40,46]
Synthetic resorbable	Guidor[38,43,48]	Sunstar Americas[38]	Polylactid acid[38,43,48]	Resorption rate: 6 weeks[38,43]
	Epi-Guide[38,40,43,46]	Curasan[38]	Poly-DL- lactic acid[40,43,46]	Resorption rate: 24-48 weeks[38,43,46]
	Resolut[38,40,46,48]	W. L. Gore & Associates[38,40]	Poly-DL- lactid/ Co-glycolid[38,40,46]	Resorption rate: 8-10weeks[38,40,46]
	Gore-TEX[40,43]	W. L. Gore & Associates[40]	Polyglycolic acid[43]	Resorption rate: 8-10 weeks[43]
	OsseoQuest[40,46]	W. L. Gore & Associates[40]	Hydrolysable polyester[40,46]	Resorption rate: 16-24 weeks[40,46]
	Biofix[40,46]	Bioscience Oy[40]	Polyglycolic acid[40,46]	Resorption rate: 24-48 weeks[40,46]
	Vicryl[40,46,48]	Johnson & Johnson[40]	Polyglactin 910 mesh[40,46,48]	Resorption rate: 4-12 weeks[40]
	Atrisorb[40,46]	Tolmar[40]	Poly-DL-lactide[40,46]	Resorption rate: 36-48 weeks[40,46]
	Vivosorb[38,40]	Polyganics[38,40]	DL-lactide-ε-caprolactone (PLCL)[38,40]	Resorption rate: < 10 weeks[38,40]

In 1991, Minabe[36] reported that for GTR purposes, absorbable membranes should maintain their structure and function in the host tissues, between 4 weeks to several months. Under that period, the membrane should not be consider biologically viable. [36] After Minabe's work, several in vivo studies were performed and several membranes were designed. [12,36]

When compared to non-absorbable membranes, the absorbable ones show some advantages. In general, absorbable membranes have the ability of stimulate the repair of soft tissues and a lower risk of additional complications, since there's no need for a second surgery.[43,49] Thereafter, the costs associated are lower.[49] The fact that they also dissolved in the oral cavity by enzymatic activity, prevents them to be contaminated by microorganisms. Instead of what happens with the non-absorbable membranes.[43]

However, there are can also be some disadvantages. Degradation process is difficult to control and depending on the type of used biopolymer, its kinetics can vary.[39,49]

The degradation process itself, can lead to a premature loss of the supportive and protective structure to the regenerated tissues.[49]

Moreover, the presence of degradation may cause a regression on the tissue regeneration due to inflammatory foreign-body responses.[3]

Collagen, the main structural protein in the ECM of biological tissues, is the "gold standard" to absorbable membranes used clinically in GTR strategies[29] [50,51] due to its high biocompatibility, good hemostatic properties, low immunogenicity and chemotactic ability to attract PDL fibroblastic cells[29].

Yet, the critical disadvantages found on these absorbable membranes,(insufficient mechanical properties, risk of cross infection[29] and unpredictable degradation profiles)[36], have led to a search for alternative materials. [29,38]

1.5 Membrane processing through Electrospinning

The basic principle behind the electrospinning technique is the application of a high voltage over a polymeric solution suspended from a needle. When the solution becomes charged, the electrostatic forces will overcome the surface tension of the solution, which allows the formation of a cone shaped structure on the tip of the syringe, named Taylor's cone. Subsequently occurs the ejection of the solution under the form of a string. As the jet travels along the electrical field, it will be orientated to hit the grounded collector, due to its opposite electrical charge. When the solution's solvent evaporates, dry polymer nanofibers will deposit in the collector under the form of a nonwoven mat. [21,42,50,52–54]

Innumerous polymers have been successfully electrospun into nanofibers, from synthetic to natural polymers for biomedical applications.

Among all the electrospun polymers studied for biomedical purposes, natural polymers are often preferred due to their enhanced biocompatibility and bifunctional motifs.[50] Currently, collagen[51,55–57], hyaluronic acid[56–58], elastin[51,55,57], fibrinogen[55], chitin[50,51,59], chitosan[42,50,51,60] and gelatin, as displayed in Table 3., seem the most promising and required biomaterials apart from silk.

Table 3 - Natural electrospun biomaterials and respective biomedical applications.

	Material	Solvent	Biomedical Purpose
Natural	Collagen[58,61–64]	HFP[58]; HFIP[58,61,64]	Tissue engineering[58,61,63]; Tooth regeneration and mucosa repair[62]
	Hyaluronic acid[58,64]	DMF[58]; Water[58,64];HCL[65]	-
	Elastin[58,63]	Water[58]	Soft tissue engineering[63]
	Fibrinogen[58,63]	HFP[58,65]	Tissue engineering[58,63]
	Chitin[58,62,63]	HFP[58,65]; HFIP[58]; PBS[58]	Vascular engineering[58]; Tooth regeneration and mucosa repair[62]; Antibacterial[63]
	Chitosan[58,62–64]	TFA[58,64]; Water[64];	Antibacterial (Caries prevention)[62,63]; Cartilage regeneration[62]; Tissue engineering[63]
	Gelatin[58,63,64]	TFE[58,64]; HFIP[58]	Tissue engineering[58,63]; Vascular grafts[63]

The obtained nanofiber-based mats, aim particular biomedical applications such as enzyme mobilization[42], drug release and delivery systems[42,66,67], tissue engineering[42,68], wound dressing[42,66,68], antibacterial materials[42] and vascular grafts.[42]

1.5.1 Silk Fibroin

Silk fibroin is widely studied and already in use for several biomaterial applications. It possesses extraordinary mechanical properties such as tensile strength, low density and an extremely ductile behavior. The unique properties of this natural material go beyond their mechanical demeanor[69,70], as it also shows some useful biological (biocompatibility[69,70], non-cytotoxicity[71], good oxygen and water vapor permeability[38,70], biodegradability[66,69,72], minimal inflammatory reaction[66,71,73] and resistance enzymatic degradation[70]) properties, besides being easy and cheap to process.[37,41,67,71]

This unique natural protein fiber, can be extracted from *Bombyx mori (B. mori)* silkworm.[72] This silk, is mainly composed of two protein components, fibroin and sericin. Sericin, which protects and binds the fibroin fibers together, must be removed to expose the silk fibroin core (Figure 7).

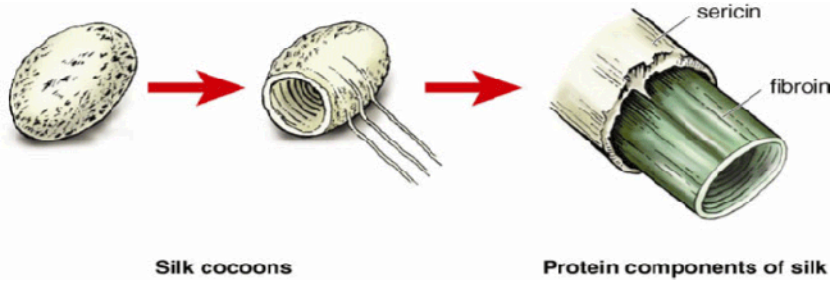

Figure 7 - Protein components of silk.[133]

Once the sericin is removed, the fibroin fibers are dissolved in an aqueous solution which can be used as a starting material in many biomaterials applications.

In its composition, silk fibroin (SF) protein is formed by an repetitive peptide segment composed by glycine (Gly), sericine (Ser) and alanine (Ala) in a molar ratio of 3:1:2 (Figure 8).[74]

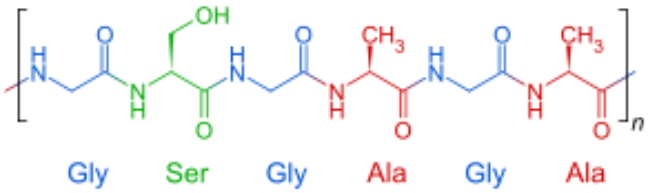

Figure 8 - Primary structure of SF.[74]

Its high glycine content allows the tight packing of the sheets, which contributes to silk's rigid structure[75] and to the remaining mechanical properties.

The SF sequence pattern, results of 3 polypeptides chains. The first two, connected by a disulfide bond (s-s), are referred as light chain (L-fibroin, with an M_w ~ 25 kD) and a heavy chain (H-fibroin), with an M_w ~ 370 kD). The third and last is a P25 glycoprotein (M_w ~ 30 kD) which associates with the first two by noncovalent interactions.

SF can contain several conformational structures: random coil, alpha helix, silk I, silk II (β-sheet) and silk III (threefold helix). For this specific fiber (*B.mori* SF) the primary structure exhibit 12 repetitive crystalline β-sheet regions plus 11 non-repetitive interspaced amorphous regions.[74] The interaction of these two distinct domains results in a hydrophobic polymer that self-assembles to form a mechanical high-performance material. Also, the β-sheet hydrophobic regions are responsible for preventing the penetration of water and proteases on the protein structure, which leads to a slower degradation of silk *in vivo*. However, after the disruption of the β-sheets, silk fibroin becomes water soluble, forming a transparent solution.

Recently SF has been recognized as a material with high potential to be processed by electrospinning technologies, since it is naturally spun by arthropods silk dope glands.[76,77] More specifically, several artificial matrices of SF and combined formulations have been produced by electrospinning for several biomedical applications[42,51,73,78], as presented in Table 4.

Table 4 - Electrospun silk fibroin blends with other polymers.

Material	Solvent	Biomedical Purpose
Silk Fibroin[58,63]	Water[65]; Formic Acid[58,63,65]; HFIP[65]; HFA[65]; Citric acid -NaOH-HCl[65]	Vascular grafts[63,65]; Wound and mucosal repair[65]; Tissue engineering[63]
Silk Fibroin/ PEO[61,65,79]	Water[61]	Scaffolds for tissue engineering[61]; GTR[62]; Bone regeneration[79]
Silk Fibroin/ P(LLA–CL)[78–80]	HFIP[80]	Scaffolds for tissue engineering[78]; Scaffolds for nerve regeneration[80]
Silk Fibroin/ PLGA[79,81]	HFIP[81]	Scaffold for ligament/tendon tissue engineering[81]
Silk Fibroin/ BMP-2[52]	Water[52]	Scaffold for bone tissue engineering[52]
Silk Fibroin/ HBS (hydroxylbutyl chitosan)[78]	HFIP/TFA[78]	Scaffolds for tissue engineering[78]
Silk Fibroin/Collagen[82]	Acetic acid[82]	Scaffolds for vascular graft engineering[82]
Silk Fibroin/Gelatin[83]	Formic acid[83]	Mats for drug release[83]
Silk Fibroin/ Hyaluronic acid[78]	Water[78]	-
Silk Fibroin/ Keratin[78]	Formic acid[78]	-
Silk Fibroin/PCL[84]	DCM/HFIP[84]	Scaffolds for tissue engineering and drug release systems[84]
Silk Fibroin-gelatin/PLA[85]	Formic solution/Chloroform and acetone[85]	Scaffolds for vascular graft engineering[85]

1.5.2 Silk Fibroin and its potential for electospinning

The electrospinning of SF, was first introduced by Zarkoob et al.[69], by reporting the formation of low concentration silk nanofibers under the influence of an electric field. The solution used, was prepared by dissolving native silk in hexafluoro-2-propanol (HFIP).[69] The silk fibroin structures generated via electrospinning, contain similar nanoscale fibers with interconnected pores which resembles the topographic features of the ECM. [86] On its native or by partially dissolved forms, SF, can be subjected to electrospinning to produce nonwoven membranes composed by fibers with diameters in the order of micro-/nanometers.

Taking into account the unique properties that SF has to offer, a wide range of applicability in several biomedical fields it's accessible. This includes hydrogels, sponges, nano-/microfibers, membranes, nanospheres and coatings that can support the repair and/or regeneration of the human tissues.[67] [68] These structures can be directly used as biomaterials for implants, scaffolds for tissue engineering and vehicles for drug release.[68] [57]

However as a natural biomaterial, silk fibroin should ideally be extracted from and processed via the production of an aqueous fibroin solution. For that, degummed silk can be dissolved in concentrated neutral salts, like lithium bromide (LiBr).[72,87,88] which can be removed through a simple process of dialysis, generating a solution, in some ways, similar to the liquid contents of a silkworm's silk gland. [54]

Following this process, the SF solution is ready to be regenerated into an electrospun mat.

Works regarding the blending of SF with other polymers have been developed, especially with polyethylene oxide (PEO).[89,90] This plasticizing agent is an amphiphilic synthetic polymer[53] usually blended into solution with other polymers to reduce the silk membrane brittleness (typical behavior in the dry state)[67,90]and improve the concentration of the native SF solutions by inducing the establishment of β-sheet conformations.[69] Besides its documented polymer biocompatibility[90] and the fact that can be easily discarded by renal and hepatic paths[53], PEO has already been successfully blended with other natural polymers, like collagen[51,90] and chitosan[53], for electrospinning.

It has been shown that the polymer concentration, plays an important role on the rheology of the solution by enhancing its viscosity. Which in turn revealed to be critical to the overall electrospinning performance and to the morphological characteristics of the obtained mats. [86] However, when considering natural biopolymers, increasing the concentration might result in several processing problems. Therefore, to blend these polymers with plasticizing polymeric additives has been a common practice.

In order to reduce the polymer blending dependence, other approaches to increase the SF processing strategy are therefore being studied.

Sonication for controlled periods of times has been already reported to increase SF viscosity by physically inducing the β-sheet crosslinking in the primary sequences. [91]

These structures permit tight packing of stacked sheets trough the establishment of hydrogen bonds between the anti-parallel chains of the protein, disulfide bonds and Van der Waals interactions. Large hydrophobic domains interspaced with smaller hydrophilic domains lead to the assembly of silk and the strength and resiliency. [67,92] [42,73] Therefore, when subjected to ultrasounds, SF accelerates the formation of this hydrophobic tightening (cross-linking) and gelation occurs.[93]

Therefore, in this work a sonication process has been introduced prior to electrospinning, to improve the spinnability of high-viscosity SF/PEO solutions and as a strategy to reduce to minimum the PEO content. If from one side the development of blends based on PEO, enable us to obtain interesting materials due to its acceptable biocompatibility and biodegradability, from the other, high proportions of this polymer can possibly became harmful to cell viability.[94]

It has been demonstrated that SF nonwoven meshes, support the adhesion, proliferation, and cell-cell interactions of a wide variety of human cell types including epithelial cells, endothelial cells, keratinocytes, osteoblasts and fibroblasts.[71] Damrongrungruang et.al[95] proved through the electrospun silkworm fibers characterization, the non-cytotoxicity of the material by observing the attachment and proliferation of gingival fibroblasts.

The fact that none of the materials currently available is ideal for dental tissue applications, alternative material as silk fibroin start being requested.[96]

II. Objectives

Therefore with this study, we intended to evaluate the added value of SF/PEO membranes for periodontal regeneration by exploring the possibility of how the use sonication process affects the viscosity of SF/PEO samples with different PEO%, in order to improve the electrospinnability of SF solutions.

In this thesis we addressed the following specific objectives:

- To investigate whether the increasing of sonication time enhances the rheological properties (viscosity) of the SF/PEO solutions.

- To compare the morphological and mechanical alterations of the electrospun mats by varying the concentration of polymer and the sonication periods.

- To assess cellular viability of PDL fibroblastic cells when in contact with the SF/PEO electrospun membranes.

III. Materials and Methods

3.1 Materials and Reagents

Silk fibroin was extracted from *Bombyx mori* cocoons provided from the Portuguese Association of Parents and Friends of Mentally Disabled Citizens (APPA-CDM, Portugal). All the remaining reagents were purchased from Sigma-Aldrich, unless stated otherwise.

3.1.1 Silk Fibroin solution preparation

Silk Fibroin from *Bombyx mori* was degummed through a previously developed procedure.[97] Briefly, silk cocoons were clean and cut into small pieces to help the dissolution process by increasing the surface contact area. After that, the cut cocoons were boiled in a solution containing 0.02 M of sodium carbonate anhydrous (Na_2CO_3; ACROS ORGANICS) for 30 minutes.

Next, the silk fibroin is rinsed for 20min and repeated 3 times (60 min total). Typically silk will lose around 20% to 30% (percentage of sericine present in raw silk fibers)[98] of its original weight.[99]

In order to produce an aqueous silk fibroin solution (native solution), first a 9.3M lithium bromide (LiBr; Sigma-Aldrich) solution was prepared. The solution was then transferred to a flask and protected from the light, since it is a photosensitive solution, by covering with aluminum foil.

SF was dissolved in the LiBr solution at 60ºC for 4hours, a ratio of SF: LiBr solution, 1:4 (wt/v).

Before the dialysis procedure starts, a piece of a dialysis membrane (snake skin dialysis tuing 10000 MWCO, Thermo Fischer Scientific), was rinsed in 1L of MiliQ water for 10 min. This step was important to humidify the membrane.

The dissolved silk fibroin was transferred to the membrane. The volume of water in which the dialysis was performed, is an important aspect and was established as 1mL of MiliQ water for 12ml of dissolved SF.

The dialysis was performed for 2 days during which the water was changed 6 times. In the first day, after 1 hour, 4 hours and before leaving. After dialysis, SF solution was centrifuged at 5000rpm for 3 periods of 20 min, at 4ºC, as a purification step.

The final concentration of SF in solution was determined by the wet weight methodology. A known volume of solution was weighted following evaporation at 60ºC overnight. Once the silk was dry, the dry weight boat was measured, obtaining the final concentration (percentage of weight per volume, wt/v). A final concentration of ~ 7% (w/v) was obtained.

3.1.2 SF/ PEO blend solutions preparation

A variety of compositions of the SF/PEO aqueous blends were prepared, which were later processed into nanofibers by electrospinning.

To increase the viscosity of the aqueous silk fibroin solution, a PEO solution was previously prepared (6 % w/v % PEO) and then mixed in different amounts to produce SF/PEO blends.

In total, three different SF/PEO blends formulations were prepared as shown in Table 5.

Table 5 - SF/PEO blend formulations prepared.

	Silk Fibroin solution (%)	PEO solution (%)
SF/ 10% PEO (wt %)	90	10
SF/ 20% PEO (wt %)	80	20
SF/ 30% PEO (wt %)	70	30

The solutions were stirred to allow the homogenization between the two polymers. Before storage, the pH of all solutions was measured to check if it was in the ideal range, between pH of 7-8. To adjust pH when necessary, solutions of hydrochloric acid (HCl) and sodium hydroxide (NaOH) were used.

All solutions were kept at 4ºC until further use.

3.2 Ultrasound Sonication

Silk fibroin/ PEO blends were sonicated with a UP50H Compact ultrasonic lab homogenizer (Hielscher-Ultrasound Technology, Germany), with power supply of 50W.

The sonication parameters were first optimized, including operating amplitude, cycle, time of sonication, type of sonotrode used and the sample volume.

These tests were performed using an indirect sonication method. Thus, the sonotrode was not put in direct contact with the sample, but with a beaker full of water (130 mL) into which the sample falcon tube was placed. All this apparatus was then put in a container with ice in order to avoid wide variations of the sample temperature, which could be caused by the ultrasounds action.

A 7 mm diameter sonotrode with a fixed amplitude of 50Hz and a continuous cycle was used. The SF/PEO samples were treated for different periods, as presented in Table 6.

Table 6- Exposure times of the SF/PEO blends to the sonication.

Blends	Sample Volume (mL)	Sonication times (min)
SF/ 10% PEO (wt %)	2,5 (for rheological assays)	0
SF/ 20% PEO (wt %)	10 (electrospinning)	7.5
SF/ 30% PEO (wt %)		15
		20

The volume of sample, the volume of water and the samples tube falcon position was always the same as shown in Figure 9.

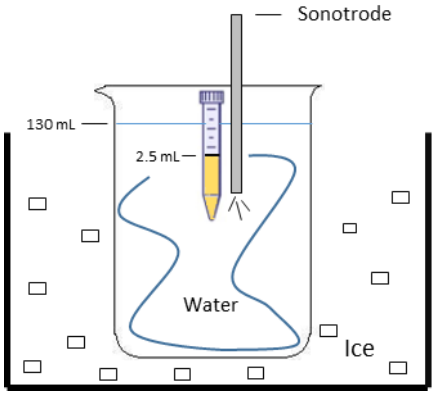

Figure 9 - Schematic diagram of sonication apparatus.

3.3 Rheological Analysis of the SF/PEO blends and native solutions

The rheological tests were performed using a rheometer (AR 2000 ex TA Instruments -USA). Before the test, the samples were subjected to a constant shear rate ($\dot{\gamma} = 10s^{-1}$) test was used in order to ensure that the samples were evenly distributed (established and uniform rheological state) along the rheometer plate.

After that, an oscillatory stepped flow assay, was used to access the rheological behavior of the solutions of SF/PEO with a linear increase of shear rate. The viscosity's "flow curves" were generated by testing the different blends over a range of shear rates. The assays were performed as shown in Table 7.

Table 7 - Rheological assays performed and respective settings.

.

Assay	Test Settings					
	Geometry	Ramp	Sample Points	Temperature (ºC)	Sample Volume (µL)	Rheometer Gap (µm)
Constant shear rate assay (Stead shear test)	20 mm crosshatched	Constant shear rate of $\Upsilon = 10s^{-1}$ for 100s	30	25	130	500
Oscillatory sweep assay (Stepped flow test)	20 mm crosshatched	Increase shear rate from $\Upsilon = 1.000s^{-1}$ to $1000\ s^{-1}$	30	25	130	500

In total, 48 samples were analyzed in the rheometer as it can be seen in Table 8.

Table 8 - SF/PEO samples formulation for rheological tests.

SF/PEO solutions	Non-sonicated (non-son)	Sonicated		
	0min	7.5min	15min	20min
0 % PEO	3 samples	0 samples	0 samples	0 samples
10% PEO	3 samples	3 samples	3 samples	3 samples
20% PEO	3 samples	3 samples	3 samples	3 samples
30% PEO	3 samples	3 samples	3 samples	3 samples

After being retrieved from the system, the obtained raw data was treated through the use of the TA Instruments TRIOS software.

3.4 Electrospinning of the Aqueous SF/PEO blends

The SF/PEO solutions were electrospun for the fabrication of SF/PEO nanofiber membranes. For each solution, 2 membranes were produced using the electrospinning equipment (Fuence Esprayer ES-2000S, Japan). The electrospinning process parameters were optimized to achieve stable spinning , in particular the flow rate, applied voltage and the distance between the tip off the syringe (a 18G tip was used) and the grounded collector.

The optimized applied voltage was 30 KV. Below this voltage, the jet formation was transient, since the electrostatic force was not high enough to overcome the surface tension. For the flow rate, a value of 20 µL/s was ideal since that for lower flor rates, the solution was ejected from the spinneret in the form of droplets. When the flow rate was higher than 20 µL/s the solution dropped onto the collector without be subjected the electrical force. Based on previous studies[100], the height of the spinneret was adjusted to 20cm, because for lower heights there is a possibility of the solvent (in this case, water) does not properly evaporate and the collected fibers end up wet.

The used electrospinning setup relies on three components. A high-voltage supplier, a capillary needle in which our polymeric solution will be inserted, and a grounded collector (aluminum foil) that have the function of collect the nanofibers.[21,42,50]

A process schematic figure is shown in Figure 10.

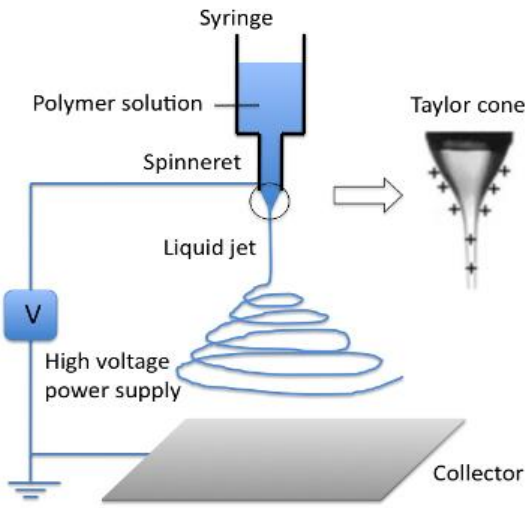

Figure 10 - Diagram of the electrospinning apparatus.[102]

Also membranes were made from had an equal volume of 9mL solution.

The obtained membranes were left in a fume hood for drying.

3.5 Morphological Characterization - Scanning Electron Microscopy (SEM)

SEM analysis of the SF membranes was performed using a Zeiss Sigma 300 (Oberkochen, Germany) scanning electron microscope SEM and a Hitachi TM3000 (Tokyo, Japan) imaging software. Samples were fixed to a copper plate using a magnesium tape. To improve the sample conductivity for the assay the membranes were treated with a 20-30nm thick copper coating prior to imaging.

The samples were analyzed at the following magnifications, x2000, x5000 and x10000 with an extra high tension (EHT) of 10.00kv.

To estimate the fiber diameter Archicad software was used. For each formulation 10 different fibers were chosen, and 3 measurements were performed along the fiber length. For this, SEM images with a magnification of 10000 x were used.

3.6 Chemical Analysis - Fourier Transform Infrared (FTIR) Spectroscopy

For the spectrum analysis, the Fourier transform infrared spectroscopy (FT-IR, PerkinElmer precisely, Spectrum 100, USA) was used to run the samples.

FTIR spectra were obtained in the range of wavenumber from 4000 to 450 cm^{-1} during 16 scans, with 4 cm^{-1} resolution. After obtaining the data, the spectrum was smoothed using the Spectrum software to minimize interferences

3.7 Mechanical Characterization - Texturometer Assay

A texturometer assay was applied for the measurement of the Ultimate Tensile Strength (UTS), Maximum Stress, Young's modulus (YM) and Elongation at break of dry and wet SF/PEO membranes. The UTS can be measured by the maximum stress that the membranes can hold while being stretched, before breaking (Figure 16). The Young´s Modulus allowed us to retrieve information on the strength that the membranes offered to elastic deformation, while the Elongation at break express the capability of our material to resist to shape changes without breaking.

5 samples - 3 cm of length (h) and 1 cm of width) of each membrane were taken and weight. Then, using a TA.XT PLUS (Texture Analyzer, UK) with a 2N load cell, the mechanical properties were evaluated by preforming a uniaxial tensile test. The samples were placed between two grips (gauge length of 100mm) and the tensile test was performed at a $1mm.s^{-1}$ speed. The obtained data was analyzed using the EXPONENT software.

3.8 Permeability Tests - Water Vapor Permeability Assay

The water vapor permeability method was performed according to the E96/E96M [ASTM, 2010].

In order to access the permeability of the SF/PEO electrospun membranes to water vapor, 3 circular samples with 1,6 cm diameter of each formulation were cut and placed on the top of glass flask after being submerged in water for 30min. MiliQ water was added until its total volume stayed 1 cm below the top. To help the adhesion of the wet membrane to the top of the flask, duct tape stick was spread over the flask borders, until the surface become sticky.

The flask was then weight on a digital scale. Measurements were registered and the samples were placed on an oven at ±35ºC. The samples were weighed and the amount of lost water was evaluated for 4 periods of time: 1, 2, 3 and 7 days.

Besides the formulations tested, a comparison with a control (flask filled with MiliQ without any cover) was also made.

3.9 Biological Tests – Cytotoxicity Assay: Direct Contact

So that the cytotoxicity of the SF/PEO membranes could be evaluated, human cells from the periodontal ligament (PDL fibroblastic cells) were first cultured for 10 in a DMEM medium complemented with 10% fetal bovine serum (FBS) and 1% Penicillin/Streptomycin under controlled conditions (37ºC, relative humidity of 95% and with a 5% CO_2 saturation). The medium was replaced regurarly. During this period, cells confluence was evaluated, until it reached a required confluence of 70% to 80%. At that moment, sterile phosphate buffered saline (PBS) solution was used to wash the cells. Trypsin/EDTA (0,25% w/v / 0,02%) was then added to allow the detachment of the cells from the bottom of the flask. After leaving the trypsin acting for two minutes, DMEM medium was used to neutralize the trypsin activity and to suspend the cells.

For the cellular contact four 48-well cell culture multiwell plates were prepared according to Figure 11. Briefly, 10000 cells/well were seeded through the suspension method in order to subject the PDL cells to direct contact with the samples for pre-defined periods of time: 1, 2, 3 and 7days.

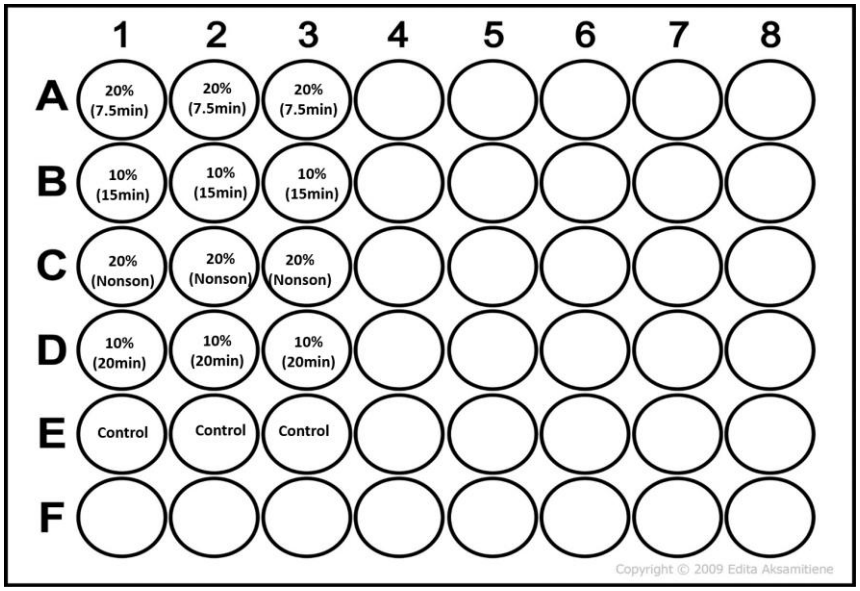

Figure 11 - 48 well plate cell culture scheme.

The 4 cell plates were incubated at 37ºC, and at each selected time point, the respective plate was removed from the incubator to prepare the samples for two freezing –thaw (Freeze – Incubate-Freeze – Incubate) cycles. These cycles promoted cell lysis occurrence, which allowed the release of the cellular content. After the 2 cycles, the lysate was ready to be tested.

A fluorescent double –stranded DNA- binding was then used according to the Quantifluor dsDNA system protocol[101], to detect the small amounts of double –stranded DNA (dsDNA) released in the cell lysis process.

Afterwards, our samples were mixed in an equal volume with a previously prepared Quantifluor dsDNA dye working solution. The samples were incubated for 5 minutes at room temperature and protected from light.

Samples were analyzed in a florescence reader (*Synergy HTX*, by *Biotek*), with excitation of 485/20 from tungsten light source at an emission of 528/20 nm.

Using the *Gen5* version 2.06 software, fluorescence data was converted to DNA concentration, and a comparison with standard curve samples was made, so that cytotoxicity of the SF/PEO membranes could be evaluated.

3.10 Statistical Analysis

One –Way analysis of variance was performed using an IBM SPSS Statistics 22 software for the mechanical characterization and permeability tests.

Statistical analyses of variance (ANOVA Two- way) analyses was performed using an IBM SPSS Statistics 22 software for the, rheological assays, cytotoxicity assays and SEM analysis of the electrospun fibers diameters.

In this study was used a 95% confidence interval, so the results were considered as statistically significant if the p-value was < 5%.

Chapter III: Results

3.1 Rheological Analysis of the SF/PEO blends and native solutions

The effect of sonication on the viscosity of the SF/PEO solutions, was assessed by rheological tests to evaluate the effect of sonication time in the solution's viscosity. The relationship between the viscosity of the samples containing 10 %, 20 % and 30 % of PEO, submitted to sonication times of 7.5, 15 and 20 min is plotted in Figure 12 and the respective average values presented on Table 9. Non-sonicated samples and native SF solution (without PEO) subjected to the same sonication times were also evaluated as control groups.

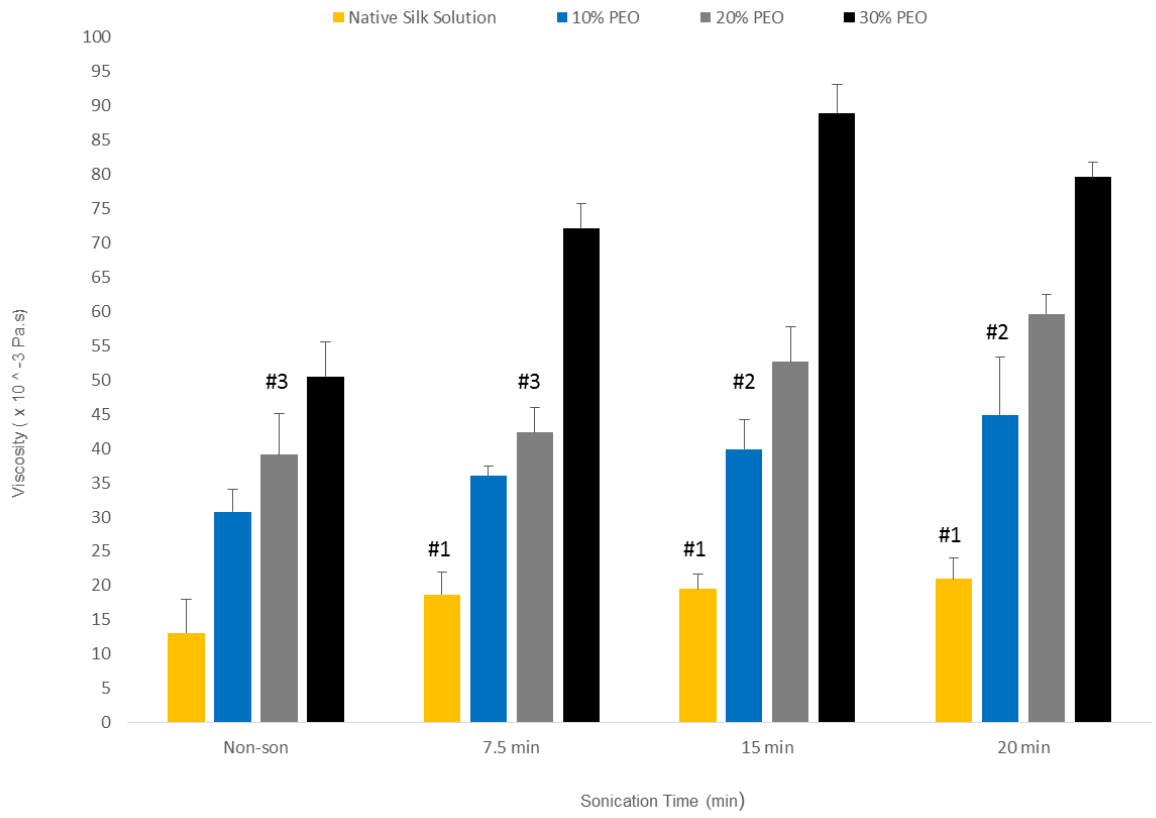

Figure 12 - Measured viscosity for all the tested SF and SF/PEO formulations as function of sonication time (min); the hashtag (#) means that no significant statistical difference was observed between the samples compared ($p>0.05$). #1 between native silk solutions; #2 between solutions with 10% of PEO; #2 between solutions with 20% of PEO.

Table 9 - Average viscosities (Pa.s) of the SF and SF/PEO solutions for increasing sonication periods.

	Sonication period (min)			
SF Solutions	**0**	**7.5**	**15**	**20**
(0% PEO)	$13.1 \pm 4.9 \times 10^{3}$	$18.7 \pm 3{,}3 \times 10^{-3}$	$19.5 \pm 2{,}2 \times 10^{-3}$	$21 \pm 3.1 \times 10^{-3}$
10% PEO	$30.8 \pm 3.3 \times 10^{3}$	$36.1 \pm 1.4 \times 10^{-3}$	$39.9 \pm 4.3 \times 10^{-3}$	$44.8 \pm 8.6 \times 10^{-3}$
20% PEO	$39.1 \pm 6 \times 10^{-3}$	$42.3 \pm 3.6 \times 10^{-3}$	$52.6 \pm 5.1 \times 10^{-3}$	$59.6 \pm 2.8 \times 10^{-3}$
30% PEO	$50.5 \pm 5.1 \times 10^{3}$	$72.1 \pm 3.6 \times 10^{-3}$	$88.9 \pm 4.2 \times 10^{-3}$	$79.6 \pm 2.2 \times 10^{-3}$

The average viscosity tends to increase, as the samples are subjected to longer sonication periods. In native silk solutions that the average viscosity of the increases from values of ~ 13.1×10^{-3} Pa.s to values of ~ 21×10^{-3} Pa.s (Table 9), before and after a sonication period of 20 minutes.

This increase is more pronounced when higher percentages of PEO are present. For example, in samples with 30 % PEO the viscosity increases from ~ 50×10^{-3} to ~ 80×10^{-3} Pa.s (Table 9) before and after a sonication period of 20 minutes, respectively.

This results indicates that the increase of viscosity by sonication is enhanced by the presence of PEO in the structure.

After testing the viscoelastic properties of the solutions, some were selected to be processed by electrospinning, accordingly to the viscosity, as presented in Table 10.

Table 10 - Formulation's viability for spinning process.

Sonication treatment	PEO (%)							
	0% (native SF)		10%		20%		30%	
	Spinning	Comments	Spinning	Comments	Spinning	Comments	Spinning	Comments
Non-sonicated	X	Viscosity too low	X	Viscosity too low	✓	Optimal viscosity for spinning	✓	Optimal viscosity for spinning
Sonicated								
7.5min	X	Viscosity too low	X	Viscosity too low	✓	Optimal viscosity for spinning	X	Viscosity too high
15min	X	Viscosity too low	✓	Formation of "beaded-fibers"	X	Solution's with similar solution already spinned	X	Viscosity too high
20min	X	Viscosity too low	✓	Optimal viscosity for spinning	✓	Optimal viscosity for spinning	X	Viscosity too high

For the non-sonicated blended solutions, only those with a minimum amount of 20 % of PEO and corresponding viscosity of $39.1 \pm 6 \times 10^{-3}$ Pa.s were able to spun in a continuous and homogeneous membrane. Nevertheless, solutions containing 10 % PEO were considered to the combined sonication and electrospinning process together with solutions containing 20 %, to evaluate whether the sonication pre-treatment could enhance the processability of solutions and/or the quality of the fibers. In the 30 % PEO blends, when submitted to sonication revealed levels of viscosity too high for electrospinning, which did not allow for the solution to flow through the spinneret.

3.2 Morphological characterization of the produced membranes

The effects of altering the solution properties via sonication pre-treatment while maintaining steady electrospinning process parameters, on the fiber formation, morphology, and diameter, were investigated macroscopically and by SEM, as presented in Figure 13. The fiber diameter was calculated for each of the conditions and plotted in Figure 14.

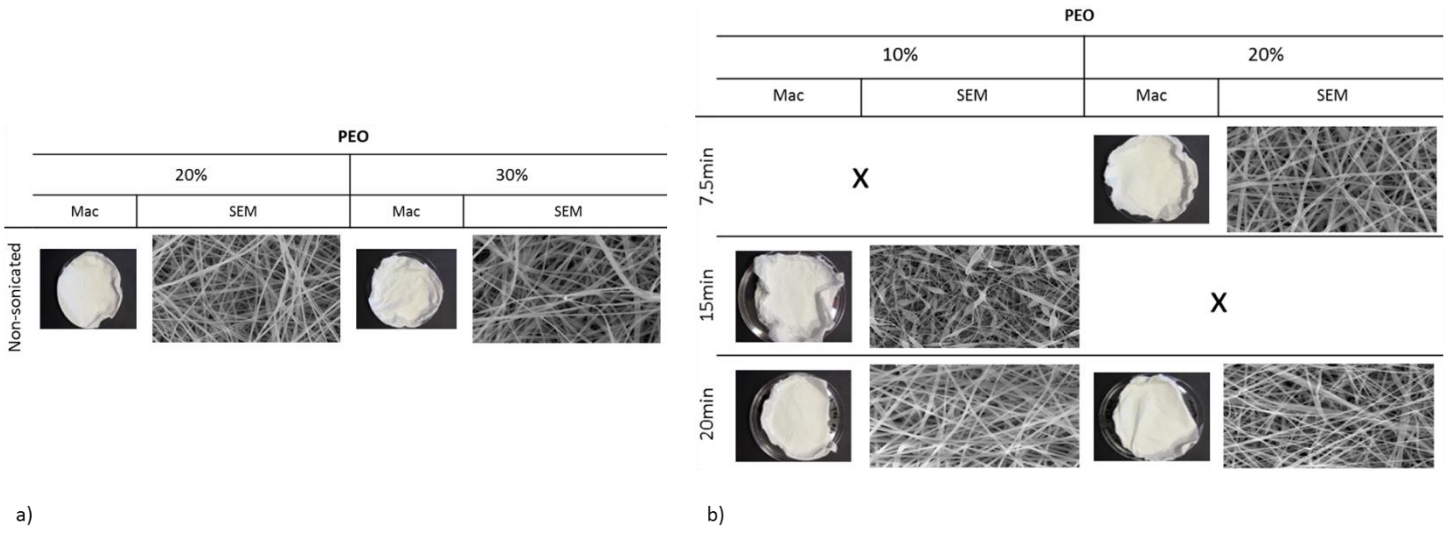

Figure 14 - Macroscopically (Mac) and SEM (SEM; magnification of 10000x) images of the samples submitted to electrospinning; a) Non-sonicated samples; b) Sonicated samples.

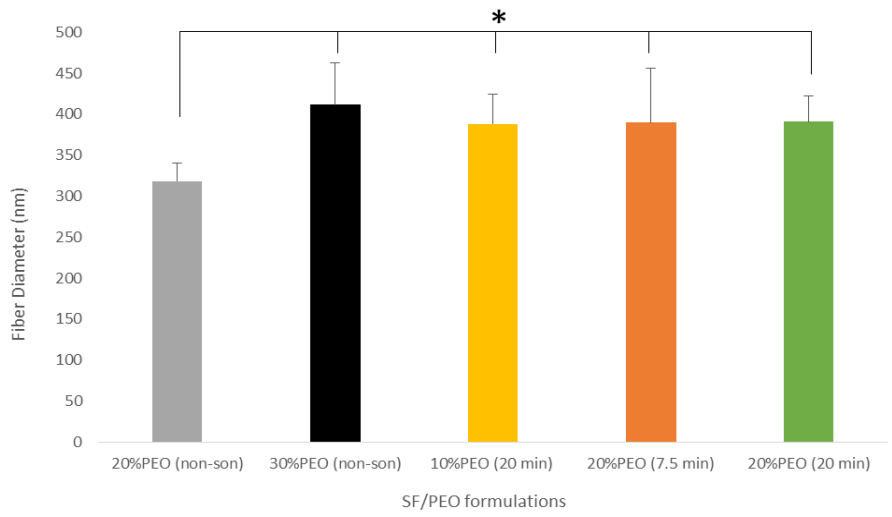

Figure 13 - Electrospun SF/PEO formulations fibers diameter plot; the asterisk (*) means that a significant statistical difference was observed between the samples compared ($p<0.05$).

The membranes produced from non-sonicated solutions containing 20 % and 30 % of PEO presented continuous fibers with uniform diameter (Figure 13. a)). When analyzing the correspondent fiber diameter (Figure 14) it is possible to observe a significant increase in the diameter ($p<0.05$) with an increase of the PEO content.

When submitting solutions to the sonication treatment prior to electrospinning it was possible to produce, as expected, viable fibers in solutions with 20 % of PEO (Figure 13. b)). The effect of sonication is visible when comparing the fiber diameters of these samples with the same without sonication.

After a sonication period of 7.5 minutes the diameter increased from ~318 ± 18 nm to ~390 ± 65 nm, which remained steady after 20 minutes (~390 ± 30 nm).

More importantly, when decreasing the percentage of PEO to 10 % and after a sonication treatment of 15 minutes it was possible to spin the solution and create a membrane, yet presenting irregular thickness and microscopically the so called “beaded-fibers”.[62,82,102] This irregularity did not allow for measuring reproducible diameter, hence its absence in Figure 14.

Nevertheless, when increasing the sonication period to 20 minutes it was possible to eliminate the bead formations and to produce continuous fibers with a regular diameter of ~388 ± 37 nm. This diameter was in the same range of the fibers produced from solutions containing 20 % PEO and sonicated for the same period (~390 ± 30 nm), indicating that the sonication period has an higher impact on the fiber diameter than the percentage of PEO.

These results demonstrate that there is a clear association between the solution composition and viscosity and the respective processability and further impact on the morphological properties of the fibers after electrospinning. Also, it was possible to select the adequate conditions. The condition that generated beaded fibers (10 % PEO and 7.5 minutes of sonication) as well as the one containing higher amount of PEO (30 %) were eliminated in further analysis conducted in this study.

3.3 Chemical Analysis - Fourier Transform Infrared (FTIR) Spectroscopy

FTIR analysis was used to study the structural changes that sonication induced on the SF/PEO electrospun membranes. Although the FTIR analysis was performed in the range of wavenumber from 4000 to 450 cm^{-1}, only the fingerprint region (1800 to 800 cm^{-1}) of the spectra corresponding to both polymers in the blend was displayed. The membranes spectra, as well as the marking of the major bands are presented in Figure 15 and Table 11.

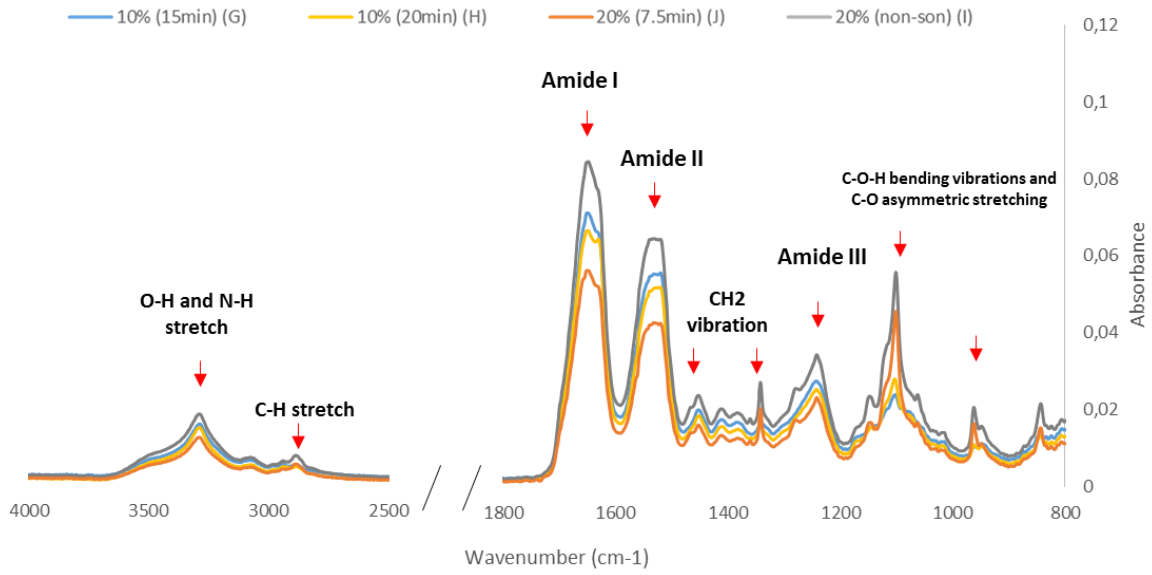

Figure 15 - FTIR spectrum of the SF/ PEO electrospun membranes.

Table 11 - Characteristic bands of the SF/PEO membranes FTIR spectrum.

Characteristic bands	Wavenumber range
C-O and C-O-H	960 cm^{-1} / 1100 cm^{-1}
Amide III	1238 - 1322 cm^{-1}
-CH2-	1348 cm^{-1} / 1460 cm^{-1}
Amide II	1500 - 1600 cm^{-1}
Amide I	1630 - 1640 cm^{-1}
C-H	2885 cm^{-1}
O-H and N-H	3200 - 3600 cm^{-1}

The spectra of all the SF/PEO membranes showed similar characteristic regions. Through the fingerprint zone (800-1800 cm^{-1}) analysis, three major characteristic bands (Figure 15) of silk fibroin were identified. A first band, amide I, appears at 1640 cm^{-1} , for the non-sonicated blend, which is characteristic of mainly amorphous silk conformation.[67,103] For the sonicated membranes, a small shoulder starts to appear at 1630 cm^{-1}, which increases with increasing time of sonication. This indicates that the sonication treatment promoted the formation of some β-sheet conformation structures.

More or less between 1500 and 1600 cm^{-1}, the FTIR spectra showed the second characteristic band of silk, the amide II, which shows no changes.[67,68,103] The last major characteristic band was the one located between 1238 to 1322 cm^{-1} known as the amide III.[67,68,103]

The bands around 1460 and 1348 cm^{-1} are attributed to the vibrations of the -CH2- group of PEO. Likewise, the bands about 1100 and 960 cm^{-1} are due the C-O group asymmetric stretching vibrations and to C-O-H bending vibrations[103] and the strong band near 2885 cm^{-1} is attributed to the symmetric and asymmetric C-H stretching.[103] It is also noticed a broad absorbance band between 3200 and 3600 $cm^{-1,}$ which is attributed to O-H and N-H groups stretching vibration.[103] These bands increase with the increasing percentages of PEO. The ratio PEO/amide I bands allow us to check this increase pattern. The samples with 10% of PEO in its composition had a ratio of 0.355 and 0.455 for the 15 minutes and 20 minutes of sonication respectively, while the 20 % PEO samples showed values of 0.719 and 0.863 for 7.5 minutes and 0 minutes respectively, using the 1100 cm^{-1} PEO peak.

3.4 Mechanical Characterization - Texturometer Assay

The mechanical tests allowed to determine the Young's Modulus, the Ultimate Tensile Strength (UTS) and the Elongation at break of the electrospun membranes in dry and wet state and are presented in Figure 16.

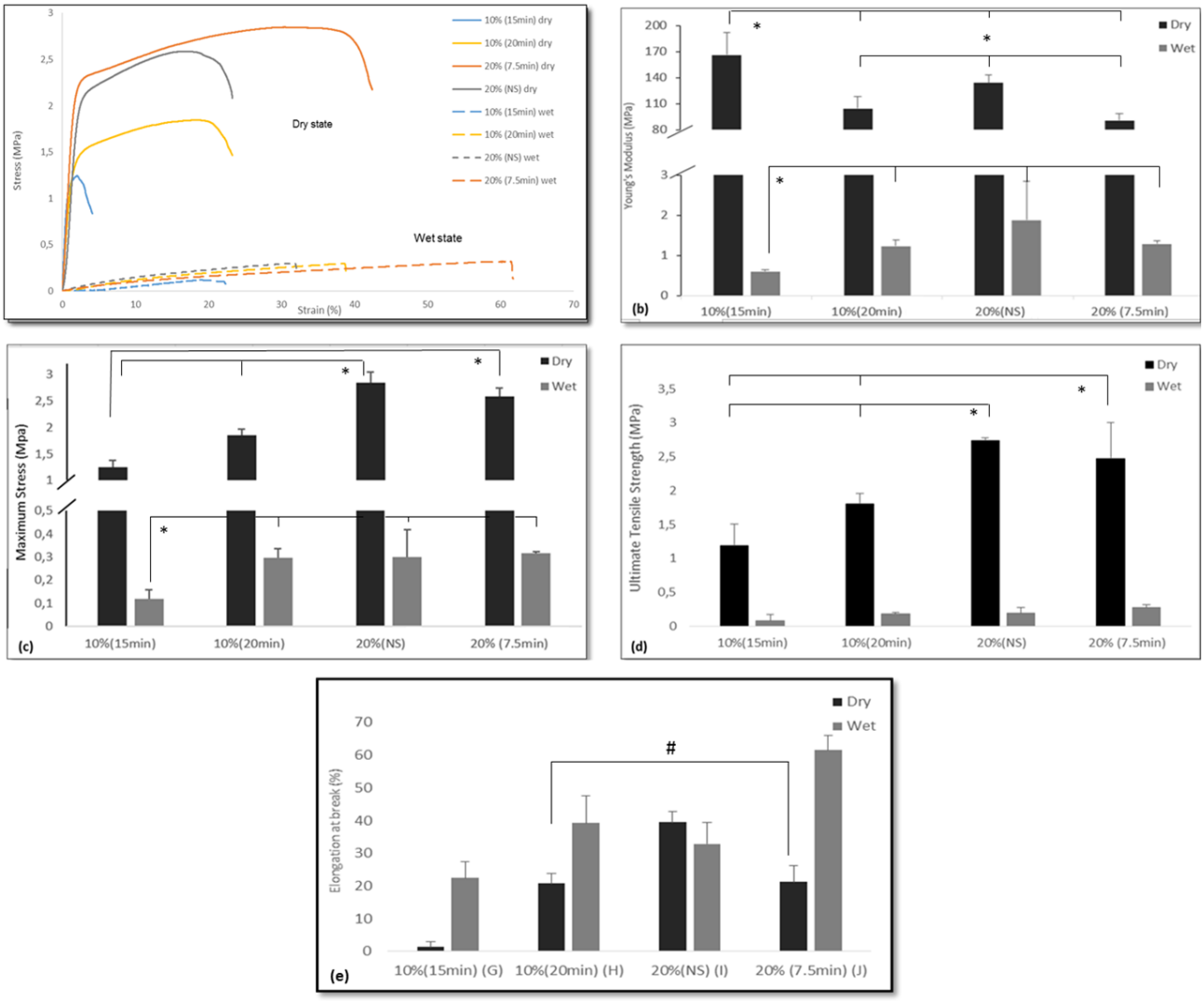

Figure 16 - Mechanical behavior of SF/PEO membranes at dry and wet states. (a) Stress-strain curves; (b) Young's Modulus; (c) Maximum stress. ; (d) Ultimate Tensile Strength (UTS); (e) Elongation at break. The asterisk (*) means that a significant statistical difference was found between the samples compared ($p < 0.05$). The hashtag (#) means that no significant statistical difference was found between the samples compared ($p > 0.05$).

The results of the mechanical tests indicate clear differences between the mechanical properties of the four membranes, mostly between dry and a wet state. In the dry state, the Young´s Modulus (Figure 16, b)) of the different samples were at least 40 times higher than those in the wet state. Maximum stress analysis also follows the same pattern, by showing that dry state samples had values at least 6 times higher than those found in the wet state. The UTS values (Figure 16, d)) showed a fold increase of 10 times higher in dry state as compared to wet state, while the elongation at break (Figure 16, e)) increases at least, to the double, indicating that the presence of water in the structure has a strong effect in plasticizing the structures of the membranes.

When comparing the different samples in the dry state, it is worth noting that formulations with the same PEO concentration, revealed lower Young´s Modulus values when submitted to the longer sonication periods. This decrease was more pronounced in the samples containing less amounts of PEO, as a result of a modification of the silk phase during sonication. The maximum stress, besides increasing with higher concentrations of PEO also increased with sonication for samples with less amount of PEO, while for the materials with 20% the values slightly decrease.

Regarding the UTS results for the dry samples it is possible to note that the samples containing higher amount of PEO (20 %) present higher tensile at break as compared with samples containing 10 % PEO. Also they are not significantly affected by the sonication treatment, while for samples containing only 20 % PEO the tensile at break increases with the time of sonication. The elongation at break increases with the sonication for both formulations and tend to be higher with increasing percentage of PEO.

In the wet state, increasing the sonication period will lead to an increase in the Young Modulus, the Maximum Stress and the UTS. At the same time the sonication period seems to have a strong effect in the elongation at break which increases with the time of elongation.

3.5 Permeability Tests - Water Vapor Permeability Assay

To study the permeability to water vapor of the SF/PEO electrospun membranes, a permeability test was performed. The results are disclosed in the Figure 17, which relates weight loss, along the different time points tested.

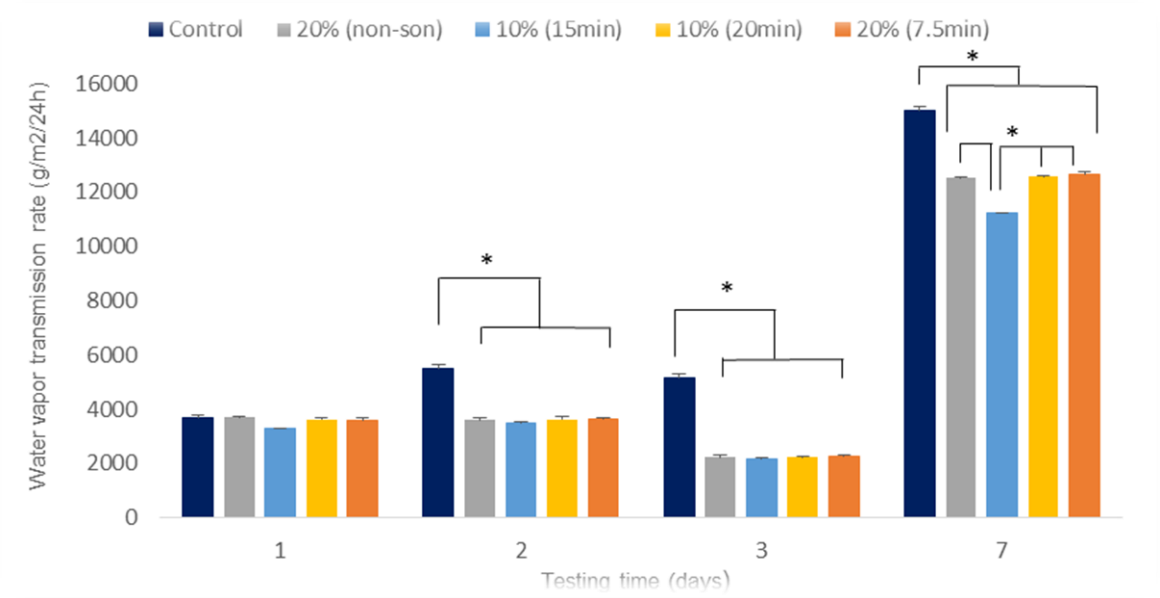

Figure 17 - Water vapor transmission rate evaluated between four time points: 1st day, 2nd day, 3rd day and 7th day; the asterisk (*) means that a significant statistical difference was observed between the samples compared and the control ($p<0.05$).

For the first three time points (day 1, day 2, day 3) water loss did not significantly differ between all four formulations. Even the control, recorded a similar water loss on the 1st day. However, from the 2nd day until the 7th day, the water transmission recorded for the control begins to be significantly ($p<0.05$) higher than that in the formulations.

After the 7th day the higher transmission rate, corresponded again to the control group. The 20 % PEO (non-son), 10 % PEO (20 min) and 20 % PEO (7.5 min) membranes also revealed the same behavior showed for the previous time points, since the weight loss was similar for the three formulations.

On the other hand, 10 % (15 min) membrane revealed a lowest weight loss of all four formulations, once the water vapor transmission was lower.

.

Nevertheless, the permeability between membranes was very similar, indicating that the mass transport is not significantly altered with increasing time of sonication or with increasing percentage of PEO. The presented values are typical for these type of nanofiber structures, as reported in the works Z.Gu et al.[104] Water vapor permeability is strongly dependent on the water diffusion coefficient.[105]

Therefore it is possible to correlate these values with capacity of the membranes to be permeable to water and biomolecules while acting as a barrier to the ligament cells. Also it opens room for other applications such as skin wound dressing, as the presented water vapor permeability is in the range of the recommended values[106] to provide an adequate level of moisture without risking wound dehydration.

These membranes will act as a cell barrier but will be permeable for the transport of nutrients and water to the ligament cells.

3.6 Biological Tests - Cytotoxicity Assay: Direct Contact

The general toxicity of the membranes was evaluated according to the DNA content on the samples. The more cytotoxic the samples are, the lower the DNA concentration (ng) present will be.

The cytotoxicity assay plot (Figure 18), showed that for the first three time points (1, 2 and 3 days), the concentration of DNA detected was similar between all the SF/PEO formulations.

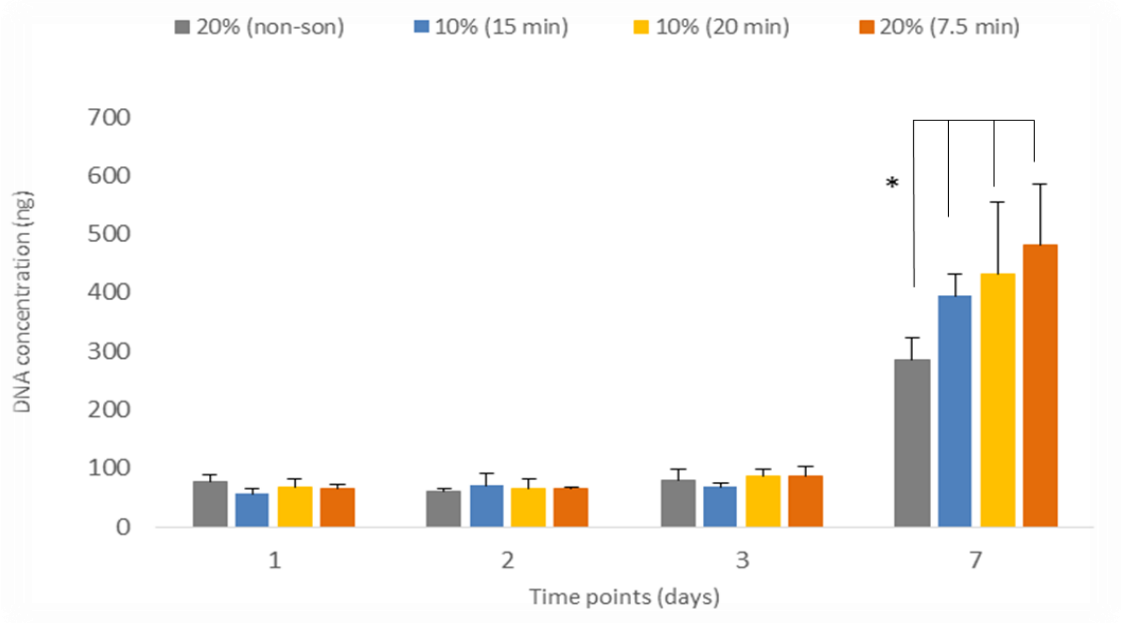

Figure 18 - dsDNA cytotoxicity assay for all the formulations. The concentration (ng) of living PDL cells was evaluated for four time points: 1st day, 2nd day, 3rd day and 7th day; the asterisk (*) means that a significant statistical difference was observed between the samples compared ($p<0.05$).

On the 7th day, the lowest DNA concentration detected corresponded to the non-sonicated sample.

It was also noted that for the 10 % PEO percentage, the DNA content was higher on the formulation that was to a longer period of sonication, 20 minutes. The 10 % PEO (20 min) formulation showed a 432.428 ± 122.968 ng DNA concentration, while the 10 % PEO (15 min) exhibited a concentration of 394.353 ± 36.578 ng.

The 20 % PEO sample that was submitted to 7.5 minutes of sonication showed the highest DNA concentration (481.072 ± 104.163 ng), and almost the double of the non-sonicated sample blended with the same PEO concentration (285.037 ± 79.102 ng).

On the other hand, this assay revealed, a sharp increase of DNA concentration from the 3rd day to the 7th for all the formulations.

Chapter 4: Discussion

At the beginning of this study, we´ve committed to evaluate whether the use of sonication would improve the electrospinning of SF/PEO solutions. In order to accomplish this, the viscosity behavior of the blends with different PEO concentrations, over sonication periods of 0, 7.5, 15 and 20 minutes was study through rheological assays. Aiming the use of the obtained mats as a GTR strategy for periodontal tissue regeneration applications, morphological and mechanical alterations of the membranes were evaluated, as a well as cytotoxicity tests to assess cellular viability of PDL cells.

Taken together, the obtained results as well as previous studies, suggest that the use of controlled periods of sonication treatment enhance the viscosity of SF/PEO solutions. Such finding, offers the possibility of reducing the use of PEO as a strategy for inducing the establishment of β-sheet conformations. Complementary tests also corroborated the sonication effect. Sonication treatment not only induced the increment fiber diameter but also the establishment of a more compact mesh capable of enhancing cell proliferation.

4.1 Rheological Analysis of the SF/PEO blends and native solutions

Rheological measurements allowed us to determine the ideal viscosity profile of SF/PEO in order to spin viable nanofibers into a membrane with adequate mechanical performance. Figure 12 shows that the rheological behavior of the SF/PEO blends was PEO dependent since, the increase of PEO concentration in solution led to significant increase in viscosity. The effect of PEO on SF solutions general viscosity enhancement had been previously reported by *Jin et al.*[76] in 2002, among others.[66,79]

Still, the objective of this study was not focused on the PEO ability to enhance silk solutions viscosity, instead, we wanted to find out if sonication, had also an important role in increasing the general viscosity as a way to decrease the amount of added synthetic polymer.

For increasing periods of sonication, the viscosity of the solutions increased, regardless of the PEO concentration blended. As the PEO concentration increase, the amplitude of the viscosity variation increases as well (Figure 12), which is in agreement with the results achieved by *V.N Kalashnikov*[108]

It is already been described in literature that sonication physically induces a conformational transition on silk, from its primitive structure (random coil) to a β-sheet conformation (silk II structure).[91,109] As previously mentioned in literature[103], SF has the ability to naturally self- assemble its random coil configuration in solution into a non-soluble β-sheet almost instantly, thus forming a more compact and stiff silk structure. Such conformational transition is also revealed when SF is exposed to several factors, such as sonication.[110]

By exposing silk fibroin to the ultrasounds treatment for a sufficient time period it was possible to induce the conformational transition in a controllable way, thus, inducing a rapid gelation. Through the adjustment in the polymer chains of the hydrophobic groups, β-sheet transition occurs, and with that, the solution's viscosity increases.[110,111]

This means that SF sol-gel transition can be accelerated through ultrasounds when small amounts of additive polymers such as PEO are present.[112]

As expected, viscosity enhancement was also confirmed, when PEO concentration increased.

Nevertheless, in solutions containing 30 % of PEO in the blend, the viscosity decreases for the longer sonication time (20 min). This can possibly be explained by the occurrence of a scission of the high chains of the polymer, for being unable to dissipate the energy imposed by the sonication as reported by *Samal et al*. [70] A disruption of SF structure happens when its major intra and inter chain interactions, as well as disulfide bonds, break. As a result, the β-sheet conformation of the silk fibroin protein was disrupted.

Gelation of solutions through ultrasounds depends, apart from polymer concentration, on the sample volume, energy output and period of sonication.[113,114] A lower energy output (lower than 50 Hz) or a larger sample volume could be possibly the ideal strategy to avoid the cleavage of the 30 % PEO blend bonds at 20 min of sonication. Thus, the obtained results, support the hypothesis that controlled sonication induces the gelation of the solution, and consequently increases viscosity.

4.2 Morphological characterization of the produced membranes

After the rheological analysis, the solutions were subjected to the electrospinning process. As described above, solution viscosity is one of the main parameters that affects the morphology of electrospun polymeric nanofibers. As described by Sell et al.[55], PEO has been used has a blending polymer to aqueous solutions in order to improve viscosity and therefore the electrospinning process.

Our experiment confirmed that the addition of PEO/sonication was required to generate silk nanofibers during the electrospinning. The relatively low molecular weight and concentration of native SF solutions did not allow a stable jet formation, being always interrupted with drops. This probably relies on the fact, that the viscosity of native SF solutions was not high enough to allow jet formation. Previous studies demonstrated that the spinning parameters defined in the present study (30 Kv of voltage, 20 µL/s of flow rate, and a plate distance of 20 cm) were not able to correctly flow native silk solutions (7 % (w/v)) through the spinneret, forming interrupted flows of nanofibers mixed with solution´s droplets, due to its low viscosity. A similar effect was found by Wang et al. for pure SF aqueous solutions at <17 % (w/v).[65] Jin et al. also recorded that a concentration >10 % (w/v) was required to the deposition of stable fibers.[90] Due to the natural SF aqueous solution low viscosity at a concentration of <10 %, which is unsuitable for spinning, Jin et al. developed in 2002 the blending technique with PEO.[90] This strategy avoids the step of concentrating the silk, which often leads to the induction of β-sheet conformation and consequent precipitation. By using this SF/PEO aqueous solution blending, it was possible to spin solutions with an original SF concentration between 3 % and 7.2 % (w/v).[90] Final SF/PEO aqueous solutions of 4.8 -8.8 % (w/v) were generated.[90] These results support the strategy herein adopted, to blend SF with different percentages of PEO.

Jet formation on the 10 % PEO (15 min) blend was also very instable. The electrospun membrane was not homogeneous as a whole, and SEM analysis revealed a nanostructure full of defects (Figure 13. b)). Polymeric solutions with low viscosity cause the formation of bead-like nanofibers, as reported for example in the works of *Quynh P.Pham et al* [86], *Z.Huang et al.*[61]*and Z.Li et al.*[115]

Still, for a similar viscosity (Table 9), the 20 % PEO (7.5 min) blend (Figure 13. b)) revealed a nanostructure also with some swellings and defects as junctions along its length. Besides low viscosity, these kind of defects, may be due the presence of water that was not able to evaporate as the jet travelled before hitting the collector.[58,62]

A higher electrical field or a lower flow rate could be solution to avoid this problem.[68] For the remaining solutions the deposited electrospun nanofibers were uniform, although junction defects were always found.

For all the experimental conditions, it was difficult to maintain a constant fiber formation throughout the fiber processing. This may be due to the fact that the electrospinning apparatus used on this study had no control of environment (humidity and temperature variations), the attractive effect of the grounded collector could not be homogeneous or even the spinning pattern not be the most appropriated could have some effect on the fiber deposition.

The diameter is a direct result of the electrospinning parameters (electric field, spinneret height and flow rate) as well as the type of polymer used.[61,66,116] Increasing the concentration of a solution, for example, is related with the increase of fiber diameter, if the solution have suitable concentration parameters for the spinning.[115] This will have a direct impact in the solution viscosity, which is a critical parameter that will influence the final electrospun fiber's morphology. Usually, a higher viscosity of the fluid jet, is a indicative of a larger fiber diameter.[61] Therefore, this justifies the studies herein conducted to evaluate in which way the concentration of PEO/sonication periods would influence the general fiber diameter of the electrospun membranes.

Sonication effect on fiber diameters was demonstrated when a comparison is made between membranes that have the same PEO concentration but with different sonication periods. General fiber diameter of samples with 20 % of PEO increased, with longer exposure times as shown in Figure 14.

The proper spin of SF/PEO blends can be related with the significantly improved rheological properties due to the sonication treatment. In agreement with Zheng-Ming Huang et al.[61] and Feng Zhang et al.[69], the enhanced viscosities of the SF/PEO blends are directly related to the formation of a stable jet and the obtainment of a continuous and smooth fibers mesh.

4.3 Chemical Analysis - Fourier Transform Infrared (FTIR) Spectroscopy

FTIR analysis, indicated that the SF/PEO membranes were mainly composed by random coil structures and that sonication induced some β-sheet conformation as demonstrated by the analysis of the amide I region (Figure 15) which presents an increase of β-sheet content, with increasing periods of sonication treatment to silk solutions. This indicates that part of the SF structure has undergone a conformation transition, which is typically accompanied by a decrease of random coils and turns as previously reported in the literature[110] Methanol/Ethanol (or other cross-linking agents) treatments are frequently used to treat electrospun membranes to induce a conformational transition from the random coil to β-sheet structures.[65,74] This cross-linking effect of some agents had been previously reported by Nogueira[67,117] et al. and Zhang et al.[65] among others.[34,41,44,48,52,79] Still, the presence of a significant amide II peak, tell us that part of the SF structure has undergone a conformation transition.

4.4 Mechanical Characterization - Texturometer Assay

The mechanical integrity play an important role in GTR, since is important to have a membrane adaptable and capable of physically support the regeneration of the surrounding tissues.

The mechanical properties of the samples follow a completely distinctive mechanical behavior in dry and wet states.

Dry samples behave predominantly as a stiff materials, however 10 % PEO (15 min) formulation (corresponds to the blue line) can already be considered to behave has a brittle material due to its ability to fracture with little or no plastic deformation.[118] Otherwise, the wet samples showed that the water molecules in the structure act as plasticizers increasing the ductility of the membranes.

As expected, dry state samples follow the opposite path by showing high Young's Modulus values and low elongation ones, which can be naturally explained not only from the lack of water that promotes ductility, but also due to the strong intermolecular forces between the polymeric structure, resulting in a more stiff material.[70]

Although the Young's Modulus wet state values were similar for all samples, the 10 % PEO (15min) sample showed slightly a lower value, in dry condition the same pattern was not followed as the 10 % PEO (15 min) sample showed the highest moduli, and therefore the lowest elongation (lowest deformability). Possibly an effect of stiffness raise due to the increment of crosslinking and β-sheet conformations as a sonication result[70] or even because it was a membrane with a structure full of defects was possible to be seen through SEM analysis.

In general, the membranes exhibited a Young's Modulus in the expected range for periodontal applications. As described Ortolani et al.[119] clinically used collagen-based membranes for dental treatment, like Jason and Collprotect, showed wet state values of 178.9 and 158.5 MPa respectively.

Susuki et al.[120] and Shadfoth et al.[121] reported that dry SF membranes without any blending and without sonication process had Young's Modulus values around 10 MPa. Our results, revealed that the highest elastic modulus value stood approximatively on the 170 MPa (10 % PEO (15 min)). H.Cao et al.[68] even reported values from 0.5 to 3 GPa for regenerated SF mats.

The absence of a post – electrospinning treatment could be the cause of some feeble mechanical properties. A greater presence of β-sheets would allow a tighter rearrangement and consequently an improvement of mechanical properties.[70] Instead, the predominance of silk on its primary structure, diminish the mechanical properties. An incomplete evaporation of solvent (water) throughout the solution ejection[122] or even high humidity[115,122] on the electrospinning chamber, would also affect the nanostructure of the membrane, and consequently the mechanical performance.

For the dry state, the UTS results came in accordance with some published studies by Suzuki et al[120]. Published UTS results were around 1-2 MPa, similar to the ones achieved for non- treated silk membranes at dry state that ranged between ~1.2 to 3MPa. This means that in dry state, SF/PEO membranes can withstand higher loads. However, Allardyce et.al[123] had substantial higher values , recording an UTS in the order of 23 to 58.8 MPa.

Noteworthy was the fact that both in dry and wet conditions, the formulations with higher PEO concentration (20 % PEO (non-son) and 20 % PEO (7.5 min)) showed higher average UTS values.

Yet, Ha et al.[124] recorded that for wet native SF membranes UTS values were close to 27.8 MPa and Allardyce et.al[123] obtained ~6.3 Mpa. Higher values in comparison with those obtained in this study. This may be due to factors adjacent to the electrospinning process, already listed above or simply for the presence of PEO.

Also, the different elongation at break presented by each of the samples allowed to confirm that the presence of the sonication treatment lead to the establishment of a more compact and rigid conformation, allowing the membrane to became less ductile.

4.5 Permeability Tests - Water Vapor Permeability Assay

This complementary test allowed to infer about the ability of the membrane to permeate biomolecules and fluids when applied to the periodontal defect and in addition allowed to get some insights on its suitability in a wound healing application.

As for the permeability, apart from the 10 % PEO (15 min), all the remaining formulations revealed similar behavior as the water vapor transmission analysis found no significant differences (p >0.05).

As described in literature, water vapor transmission of uncovered human dermis wounds, it's around 4800g/m^2/ 24h.[104] Wound healing requires an ideal level of moisture in order to control the regeneration environment, but also to minimize the risk of infection.[104,125] The transmission rate should not be too high, to avoid dehydration problems whereas no too low to avoid an excessive accumulation of exudates.[104,126]

The fact that the higher diffusion rate corresponds to the control group was already expected, since there was no barrier (membrane) covering the top of the flask. 10 % PEO (15 min) membrane revealed less permeability to water vapor. It is perceptible that at the 7th day, the water vapor transmission was lower than the other samples. Suggesting a less water loss. This could be related to the membrane porous nanostructure. A regular and oriented nanofiber deposition, created a structure with a large and well-defined porosity for the 20 % PEO (non-son), 10 % PEO (20 min) and 20 % PEO (7.5 min) membranes. However, for the 10 % PEO (15 min), an instability on fiber deposition and the irregular fiber diameter of the fibers due to defects “beaded” defects, created an electrospun mesh more thigh and therefore more waterproof than the others.

Wharram et a.l electrospun silk studies[125] showed that water vapor transmission of hydrated membranes values ranged between ~1900 and 2100 g/m^2/24h. Similar results were obtained by Z.Xu et al. regarding SF/chitosan membranes.[127] Closer results to ours, were obtained by Z.Gu et al. with wound dressing studies performed with SF/chitosan membranes fixed with alginate dialdheyde.[104] After 24h Z.Gu et al. membranes showed a water vapor transmission range between ~2500 to 3500 g/m^2/24h, similar to the ~3500 to 4000 g/m^2/24h range that we had after the 24hours.
Such differences between our results and literature it may be attributed to the material properties like fiber size, thickness, porosity and fiber density.[125]

Although the obtained values appear to be somewhat elevated when comparing to previous studies and with commercial polymer films[128], is important to stress that water vapor transmission of the oral mucosa is probably higher than the one on the dermis, which make the membranes suitable to periodontal use.

4.6 Biological Tests - Cytotoxicity Assay: Direct Contact

According to the cytoxicity assays, statistical analysis revealed that between the four formulations studied, statistically significant differences were only found at the 7th day ($p < 0.05$).

The analysis revealed a massive increase of DNA content for all membranes between the 3rd and the 7th day, although, throughout the first three time points, absence of cellular growth was evident, since no statistical difference of DNA content was noticed. Cellular adaptation to the membrane could be one explanation. The presence of PEO on the membrane structure may had been responsible by inhibiting cell attachment on the first days.[55] When the cells attached to the surface, the proliferation was evident (Figure 17.)

Even in the absence of a control group (mistakenly the control group was not added to the cell culture plate) it is clear, the lack of toxicity. Unlike what´s suggested by *Sell et all.*[55], PEO has shown to have no harmful effect on cell viability. Between all four formulations, only the 20 % PEO (non-son) showed a lower DNA content. Maybe because some residual ethanol that was no properly removed after the sterilization of membranes. A poor homogenization of the culture in cell passage process, the influence of external parameters, as temperature variation, the depletion of nutrients or even toxic action of cell metabolism products could also be related to this dissimilarity.

Chapter 5: Conclusions and Future Perspectives

The present developed work constitutes a step forward towards the processing of viable electrospun SF-based membranes for periodontal regeneration since it demonstrates that it is possible to tune the viscosity of SF solutions to achieve optimal processing conditions using a simple sonication step prior to the electrospinning process, minimizing the amount of synthetic polymer to be used.

Future work should focus on the study of other ultrasound power output as well as other sonication periods of exposure. Lower PEO concentrations on the SF/PEO blends should be also taken into account. The same applies to the electrospinning process. In order to obtain a proper spinning of the SF/PEO blends, the spinning process parameters (the electric field applied, the flow rate and the distance between the spinneret and the grounded collector) should be further investigated. In high-viscosity samples (30% PEO blends) the spinning process was difficult to preform, since the spinneret tip was constantly being blocked, preventing the solution from flowing normally. The fact that the electrospinning apparatus had no humidity and temperature control, it may also influenced the arrangement of fiber deposition, originating non-homogeneous meshes. Thickness and porosity size measurements should be something to consider in future studies for a better understanding of the electrospinning parameters.

Aiming a periodontal application, satisfactory mechanical properties were also achieved, with the samples in dry and wet states, following a predictable outcome of distinctive mechanical behavior. However, some of the properties evaluated, like UTS, exhibited results somewhat lower than those found in literature. Such feeble properties, could be related to the absence of an electrospinning post-treatment. During the electrospinning process, water (was used as a solvent), possibly did not had enough time to volatilize, remaining in the membrane. Thus, the membrane is usually treated with ethanol/methanol to induce a conformational transition. Chemical analysis proved this, by revealing a high amide I peak (amorphous conformation).

Permeability and biological complementary tests also revealed the promissory effect of these membranes as a biocompatible and well functioned biomaterial able to mimic the natural ECM. Still, MTT and Live-Dead tests are currently being planned for further cell viability analysis.

Antimicrobial studies should be performed to study whether the membranes prevent the proliferation of microorganisms.

Despite the latest developments, silk-based materials for dentistry applications has only recently begun. Silk presents several desirable characteristics for biomedical applications, being able to compete with traditionally used materials. There is still a long way to go, several problems need to be solved, but still silk arises as a promisor material for dental applications.

References

1. Park, C., Kim, K.-H., Lee, Y.-M. & Seol, Y.-J. Advanced Engineering Strategies for Periodontal Complex Regeneration. *Materials (Basel).* **9,** 57 (2016).
2. Deka, N. Tissue engineering approach for periodontal regeneration. **1,** 71–74 (2015).
3. Lindhe, J. *Clinical Periodontology and Implant Dentistry Volume 2*. (2008).
4. Shimauchi, H., Nemoto, E., Ishihata, H. & Shimomura, M. Possible functional scaffolds for periodontal regeneration. *Jpn. Dent. Sci. Rev.* **49,** 118–130 (2013).
5. Gakhar, A. Macroscopic Structures of Gingiva. 57 (2012). Available at: http://www.slideshare.net/abhishekgakhar11/seminar1-35776648.
6. Palumbo, a. The Anatomy and Physiology of the Healthy Periodontium. *Gingival Dis. - Their Aetiol. Prev. Treat.* 3–22 (2011).
7. Bartold, P. M. & Bartold, P. M. Periodontal tissues in health and disease: introduction. *Periodontol. 2000* **40,** 7–10 (2006).
8. Williams, R. C. & Genco, R. J. *Periodontal Disease and Overall Health : A Clinician ' s Guide Editors Periodontal Disease and Overall Health : A Clinician ' s Guide*. *Medicine* (2010).
9. Genco, R. J. & Borgnakke, W. S. Risk factors for periodontal disease. *Periodontol. 2000* **62,** 59–94 (2013).
10. Hasan, A. & Palmer, R. M. A clinical guide to periodontology: Pathology of periodontal disease. *Bdj* **216,** 457–461 (2014).
11. Guidance, D. C. Scottish Dental Clinical Effectiveness Programme Prevention and Treatment of Periodontal Diseases in Primary Care Dental Clinical Guidance. (2014).
12. Joshi, D., Garg, T., Goyal, A. K. & Rath, G. Advanced drug delivery approaches against periodontitis. *Drug Deliv.* **00,** 1–15 (2014).
13. Oral complications of Type 1 diabetes mellitus in a non-smoking population. (2011).
14. Pejcic, A., Kojovic, D., Mirkovic, D. & Minic, I. Stem cells for periodontal regeneration. *Balkan J. Med. Genet.* **16,** 7–12 (2013).
15. Angelica, M. D. & Fong, Y. NIH Public Access. *October* **141,** 520–529 (2008).
16. Group, O. Treatment of Plaque-induced Gingivitis , Chronic Periodontitis , and Other Clinical Conditions. **36,** 360–369 (2004).
17. Group, O. Guideline for Periodontal Therapy. (2003).
18. London, R. Periodontal Flap Surgery. *Dear Doctor - Dentistry & Oral Health* 4 (2010).
19. Services, H. Periodontal (Gum) Disease.
20. Alghamdi, H., Babay, N. & Sukumaran, A. Surgical management of gingival recession : A clinical update. *Saudi Dent. J.* **21,** 83–94 (2009).
21. Rasperini, G. Surgical approaches based on biological objectives: GTR vs GBR techniques. *Int. J. Dent.* **2013,** (2013).
22. Yu, S. *et al.* Effect of fibroblast growth factor on injured periodontal ligament and cementum after tooth replantation in dogs. 111–119 (2015).

23. Albrektsson, T., Zarb, G., Worthington, P. & Eriksson, A. R. The long-term efficacy of currently used dental implants: a review and proposed criteria of success. *Int. J. Oral Maxillofac. Implants* **1,** 11–25 (1986).
24. Manuscript, A. Growth factor delivery for oral and periodontal tissue engineering. *October* **3,** 647–662 (2008).
25. Bartold, P. M., Gronthos, S., Ivanovski, S., Fisher, A. & Hutmacher, D. W. Tissue engineered periodontal products. *J. Periodontal Res.* **51,** 1–15 (2016).
26. Bottino, M. C. *et al.* Recent advances in the development of GTR/GBR membranes for periodontal regeneration - A materials perspective. *Dent. Mater.* **28,** 703–721 (2012).
27. Zhu, W. & Liang, M. Periodontal ligament stem cells: Current status, concerns, and future prospects. *Stem Cells Int.* **2015,** (2015).
28. Lin, N. H., Gronthos, S. & Mark Bartold, P. Stem cells and future periodontal regeneration. *Periodontol. 2000* **51,** 239–251 (2009).
29. Aurer, A. & JorgiE-Srdjak, K. Membranes for Periodontal Regeneration. *Acta Stomatol. Croat.* **39,** 107–112 (2005).
30. Nyman, S., Gottlow, J., Karring, T. & Jan, L. The regenerative potential of the periodontal ligament. *J. Clin. Periodontol.* (1982).
31. Gottlow, J. A. N., Nyman, S., Karring, T. & Lindiit, J. A. N. New attachment formation as the result of controlled tissue regeneration. 494–503 (1984).
32. Isidor, F., Karring, T., Nyman, S. & Lindhe, J. The significance of coronal growth of periodontal ligament tissue for new attachment formation. *J. Clin. Periodontol.* **13,** 145–150 (1986).
33. Manuscript, A. repair. **59,** 185–202 (2013).
34. Pisoschi, C., Stanciulescu, C. & Banita, M. Growth Factors and Connective Tissue Homeostasis in Periodontal Disease. (2012). doi:10.5772/1159
35. Wahl, S. M. Transforming growth factor beta (TGF-beta) in inflammation: a cause and a cure. *J. Clin. Immunol.* **12,** 61–74 (1992).
36. Singh, A. K. GTR membranes : The barriers for periodontal regeneration. **4,** 31–38 (2013).
37. Sang-Woon Lee, and S.-G. K. Membranes for the Guided Bone Regeneration. *Maxillofac. Plast. Reconstr. Surg.* **36,** 239–246 (2014).
38. Wang, J. *et al.* Biodegradable Polymer Membranes Applied in Guided Bone/Tissue Regeneration: A Review. *Polymers (Basel).* **8,** 115 (2016).
39. Nair, L. S. & Laurencin, C. T. Biodegradable polymers as biomaterials. *Prog. Polym. Sci.* **32,** 762–798 (2007).
40. Zhang, Y., Zhang, X., Shi, B. & Miron, R. J. Membranes for guided tissue and bone regeneration. 1–10 (2013).
41. Lu, S. *et al.* Original Article A novel silk fibroin nanofibrous membrane for guided bone regeneration : a study in rat calvarial defects. **7,** 2244–2253 (2015).
42. Yukseloglu, S. M., Sokmen, N. & Canoglu, S. Biomaterial applications of silk fibroin electrospun nanofibres. *Microelectron. Eng.* **146,** 43–47 (2015).
43. Soheilifar, S., Soheilifar, S., Bidgoli, M. & Torkzaban, P. Barrier Membrane, a Device for

Regeneration: Properties and Applications. *Avicenna J. Dent. Res.* **6,** (2014).

44. Donos, N. Alveolar ridge augmentation by combining autogenous mandibular bone grafts and non-resorbable membranes An experimental study in the rat. 185–191 (1995).
45. Schneider, D., Jung, R. E., Thoma, D. S. & Thoma, D. S. Randomized clinical study assessing two membranes for guided bone regeneration of peri-implant bone defects : clinical and histological outcomes at 6 months. 1–9 (2016). doi:10.1111/clr.12977
46. Dwi, Y., Dds, R., Dds, Y. A., Dds, A. F. & Dds, K. K. Current barrier membranes : Titanium mesh and other membranes for guided bone regeneration in dental applications. *J. Prosthodont. Res.* **57,** 3–14 (2013).
47. Dimitriou, R., Mataliotakis, G. I., Calori, G. M. & Giannoudis, P. V. The role of barrier membranes for guided bone regeneration and restoration of large bone defects : current experimental and clinical evidence. *BMC Med.* **10,** 81 (2012).
48. Hitti, R. A. & Kerns, D. G. Guided Bone Regeneration in the Oral Cavity : A Review. 33–45 (2011).
49. Gbr, R. Otolaryngology and Rhinology ClinMed. 1–8 (2015).
50. Gu, P., Joseph, M. M., Bs, U., Shiji, R. & Tt, S. Biomedical Applications of Natural Polymer Based Nanofibrous Scaffolds. *Int. J. Med. Nano Res.* (2015).
51. Sionkowska, A. Current research on the blends of natural and synthetic polymers as new biomaterials : Review. *Prog. Polym. Sci.* **36,** 1254–1276 (2011).
52. Li, C., Vepari, C., Jin, H.-J., Kim, H. J. & Kaplan, D. L. Electrospun silk-BMP-2 scaffolds for bone tissue engineering. *Biomaterials* **27,** 3115–24 (2006).
53. Liang, D., Hsiao, B. S. & Chu, B. Functional Electrospun Nanofibrous Scaffolds for Biomedical Applications. *Adv. Drug Deliv. Rev. Deliv.* **59,** 1392–1412 (2007).
54. Wang, M., Jin, H.-J., Kaplan, D. L. & Rutledge, G. C. Mechanical Properties of Electrospun Silk Fibers. *Macromolecules* **37,** 6856–6864 (2004).
55. Sell, S. A. *et al.* The use of natural polymers in tissue engineering: A focus on electrospun extracellular matrix analogues. *Polymers (Basel).* **2,** 522–553 (2010).
56. Fischer, R. L., Mccoy, M. G. & Grant, S. A. Electrospinning collagen and hyaluronic acid nanofiber meshes. (2012). doi:10.1007/s10856-012-4641-3
57. Zhao, Z., Li, Y. & Xie, M. Bin. Silk fibroin-based nanoparticles for drug delivery. *Int. J. Mol. Sci.* **16,** 4880–4903 (2015).
58. Haider, A., Haider, S. & Kang, I. A comprehensive review summarizing the effect of electrospinning parameters and potential applications of nanofibers in biomedical and biotechnology. *Arab. J. Chem.* (2015). doi:10.1016/j.arabjc.2015.11.015
59. Min, B. *et al.* Chitin and chitosan nanofibers : electrospinning of chitin and deacetylation of chitin nanofibers. **45,** 7137–7142 (2004).
60. Ojha, S. S. *et al.* Fabrication and Characterization of Electrospun Chitosan Nanofibers Formed via Templating with Polyethylene Oxide. 2523–2529 (2008).
61. Huang, Z. M., Zhang, Y. Z., Kotaki, M. & Ramakrishna, S. A review on polymer nanofibers by electrospinning and their applications in nanocomposites. *Compos. Sci. Technol.* **63,** 2223–

2253 (2003).
62. Zafar, M., Najeeb, S., Khurshid, Z., Vazirzadeh, M. & Zohaib, S. Potential of Electrospun Nanofibers for Biomedical and Dental Applications. *Materials (Basel).* 1–21 (2016). doi:10.3390/ma9020073
63. Agarwal, S., Wendorff, J. H. & Greiner, A. Use of electrospinning technique for biomedical applications. *Polymer (Guildf).* **49,** 5603–5621 (2008).
64. Leung, V. & Ko, F. Biomedical applications of nanofibers. (2011). doi:10.1002/pat.1813
65. Zhang, X., Reagan, M. R. & Kaplan, D. L. Electrospun silk biomaterial scaffolds for regenerative medicine ☆. *Adv. Drug Deliv. Rev.* **61,** 988–1006 (2009).
66. Dou, H. & Zuo, B. Q. Effect of Sodium Carbonate Concentrations on the Formation and Mechanism of Regenerated Silk Fibroin Nanofibers by Electrospinning. *J. Nanomater.* **2014,** (2014).
67. Nogueira, G. M. *et al.* Preparation and characterization of ethanol-treated silk fibroin dense membranes for biomaterials application using waste silk fibers as raw material. *Bioresour. Technol.* **101,** 8446–8451 (2010).
68. Cao, H., Chen, X., Huang, L. & Shao, Z. Electrospinning of reconstituted silk fiber from aqueous silk fibroin solution. *Mater. Sci. Eng. C* **29,** 2270–2274 (2009).
69. Zhang, F. *et al.* Mechanisms and control of silk-based electrospinning. *Biomacromolecules* **13,** 798–804 (2012).
70. Samal, S. K., Kaplan, D. L. & Chiellini, E. Ultrasound sonication effects on silk fibroin protein. *Macromol. Mater. Eng.* **298,** 1201–1208 (2013).
71. Woo, H. *et al.* Wound healing effect of electrospun silk fibroin nanomatrix in burn-model. *Int. J. Biol. Macromol.* **85,** 29–39 (2016).
72. Rajkhowa, R., Tsuzuki, T. & Wang, X. G. Recent Innovations in Silk Biomaterials. *Text. Bioeng. Informatics Symp. Proceedings, Vols 1-3* 583–593 (2010). doi:Doi 10.3993/Tbis2010103
73. Lawrence, B. D. Processing of Bombyx mori for biomedical applications. *Silk Biomater. Tissue Eng. Regen. Med.* 78–99 (2014). doi:10.1533/9780857097064.1.78
74. Fallis, A. . Silk Fibroin. *J. Chem. Inf. Model.* **53,** 1689–1699 (2013).
75. Nagwa, W. I. A. & Ghareib, A. Influence of the protocol of fibroin extraction on the antibiotic activities of the constructed composites. *Prog. Biomater.* **4,** 77–88 (2015).
76. Mortimer, B., Guan, J., Holland, C., Porter, D. & Vollrath, F. Linking naturally and unnaturally spun silks through the forced reeling of Bombyx mori. *Acta Biomater.* **11,** 247–255 (2015).
77. Li, G. *et al.* The natural silk spinning process. **6606,** 6600–6606 (2001).
78. Zhang, J. G. & Mo, X. M. Current research on electrospinning of silk fi broin and its blends with natural and synthetic biodegradable polymers. **7,** 129–142 (2013).
79. Li, Z.-H., Ji, S.-C., Wang, Y.-Z., Shen, X.-C. & Liang, H. Silk fibroin-based scaffolds for tissue engineering. *Front. Mater. Sci.* **7,** 237–247 (2013).
80. Wang, C. *et al.* Aligned natural – synthetic polyblend nanofibers for peripheral nerve regeneration. *Acta Biomater.* **7,** 634–643 (2011).
81. Sahoo, S., Lok, S. & Goh, J. C. H. A bFGF-releasing silk / PLGA-based biohybrid scaffold for

ligament / tendon tissue engineering using mesenchymal progenitor cells. *Biomaterials* **31,** 2990–2998 (2010).

82. Zhou, J., Cao, C., Ma, X. & Lin, J. Electrospinning of silk fibroin and collagen for vascular tissue engineering. *Int. J. Biol. Macromol.* **47,** 514–519 (2010).
83. Okhawilai, M., Rangkupan, R., Kanokpanont, S. & Damrongsakkul, S. Preparation of Thai silk fibroin / gelatin electrospun fiber mats for controlled release applications. *Int. J. Biol. Macromol.* **46,** 544–550 (2010).
84. Li, L. *et al.* Electrospun poly (e-caprolactone)/silk fibroin core-sheath nanofibers and their potential applications in tissue engineering and drug release. *Int. J. Biol. Macromol.* **49,** 223–232 (2011).
85. Wang, S., Zhang, Y., Wang, H., Yin, G. & Dong, Z. Fabrication and Properties of the Electrospun Polylactide / Silk Fibroin-Gelatin Composite Tubular Scaffold. *Biomacromolecules* 2240–2244 (2009).
86. Pham, Q. P., Sharma, U. & Mikos, A. G. Electrospinning of Polymeric Nanofibers for Tissue Engineering Applications : A Review. **12,** (2006).
87. Sah, M. K., Pramanik, K. & Materials, a. Regenerated Silk Fibroin from B . mori Silk Cocoon for Tissue Engineering Applications. *nternational J. Environ. Sci. Dev.* **1,** 404–408 (2010).
88. Kameda, T. Influence of pH, temperature, and concentration on stabilization of aqueous hornet silk solution and fabrication of salt-free materials. *Biopolymers* **103,** 41–52 (2015).
89. Fomby, P. & Cherlin, A. J. NIH Public Access. **72,** 181–204 (2011).
90. Jin, H., Fridrikh, S. V, Rutledge, G. C. & Kaplan, D. L. Electrospinning Bombyx mori Silk with Poly (ethylene oxide). 1233–1239 (2002).
91. Brown, J., Lu, C. L., Coburn, J. & Kaplan, D. L. Impact of silk biomaterial structure on proteolysis. *Acta Biomater.* **11,** 212–221 (2015).
92. Kaplan, D. L., Hu, X., Lu, Q., Kaplan, D. L. & Cebe, P. Microphase Separation Controlled β - Sheet Crystallization Kinetics in Fibrous Proteins Fibrous Proteins. (2009). doi:10.1021/ma802481p
93. Doyle, I. M. P., Dale, G., Choi, H. & City, B. (12) UnIted States Patent. **2,** (2012).
94. Ang, H. Y. *et al.* Characterization of a bioactive fiber scaffold with entrapped HUVECs in coaxial electrospun core- shell fiber Characterization of a bioactive fiber scaffold with entrapped HUVECs in coaxial electrospun core-shell fiber. **2535,** (2014).
95. Fibroblast, G. & Prelimi, A. Fabrication of electrospun thai silk fibroin nanofiber Fabrication of Electrospun Thai Silk Fibroin Nanofiber and lts Effect on Human. (2016).
96. Zafar, M. S. & Al-Samadani, K. H. Potential use of natural silk for bio-dental applications. *J. Taibah Univ. Med. Sci.* **9,** 171–177 (2014).
97. Yan, L. *et al.* Macro / microporous silk fibroin scaffolds with potential for articular cartilage and meniscus tissue engineering applications. *Acta Biomater.* **8,** 289–301 (2012).
98. S.Wray, L. *et al.* Effect of Processing on Silk-Based Biomaterials: Reproducibility and Biocompatibility. *J. Biomed. Mater. Res. - Part B Appl. Biomater.* **99B,** 89–101 (2011).
99. Choudhury, M., Talukdar, B. & Devi, D. Surface smoothening and characterization of silk fibers

of Antheraea assamensis Helfer (muga) using some natural agents. *J. Text. Inst.* **5000,** (2015).

100. Hodgkinson, T., Chen, Y., Bayat, A. & Yuan, X. F. Rheology and electrospinning of regenerated Bombyx mori silk fibroin aqueous solutions. *Biomacromolecules* **15,** 1288–1298 (2014).
101. Promega. QuantiFluor ® dsDNA System QuantiFluor ® dsDNA System. *Tech. Man.* (2015).
102. Athira, K. S., Sanpui, P. & Chatterjee, K. Fabrication of Poly(Caprolactone) Nanofibers by Electrospinning. *J. Polym. Biopolym. Phys. Chem.* **2,** 62–66 (2014).
103. Laity, P. R., Gilks, S. E. & Holland, C. Rheological behaviour of native silk feedstocks. *Polym. (United Kingdom)* **67,** 28–39 (2015).
104. Gu, Z., Xie, H., Huang, C., Li, L. & Yu, X. Preparation of chitosan / silk fibroin blending membrane fixed with alginate dialdehyde for wound dressing. *Int. J. Biol. Macromol.* **58,** 121–126 (2013).
105. Muller, C. M., Laurindo, J. B. & Yamashita, F. Effect of cellulose fibers addition on the mechanical properties and water vapor barrier of starch-based films. *Food Hydrocoll.* **23,** 1328–1333 (2009).
106. Lamke, L., Nilsson, G. E. & Reithner, H. L. The evaporative water loss from burns and the water-vapour permeability of grafts and artificial membranes used in the treatment of burns. (1970).
107. Ekemen, Z., Ahmad, Z., Stride, E., Kaplan, D. & Edirisinghe, M. Electrohydrodynamic bubbling: An alternative route to fabricate porous structures of silk fibroin based materials. *Biomacromolecules* **14,** 1412–1422 (2013).
108. Kalashnikov, V. N. Shear-rate dependent viscosity of dilute polymer solutions. *J. Rheol. (N. Y. N. Y).* **38,** 1385 (1994).
109. Wang, H.-Y. & Zhang, Y.-Q. Effect of regeneration of liquid silk fibroin on its structure and characterization. *Soft Matter* 138–145 (2012). doi:10.1039/c2sm26945g
110. Wang, X., Kluge, J. A., Leisk, G. G. & Kaplan, D. L. Sonication-induced gelation of silk fibroin for cell encapsulation. **29,** 1054–1064 (2008).
111. Matsumoto, A. *et al.* Mechanisms of Silk Fibroin Sol - Gel Transitions. 21630–21638 (2006).
112. Wang, Xiaoqin; Kluge, Jon; Leisk, Gary; Kaplan, D. . Method for silk fibroin gelation using sonication. (2014).
113. Wang, X., Kluge, J., Leisk, G. G. & Kaplan, D. L. NIH Public Access. **29,** 1054–1064 (2009).
114. Wang, I. X. *et al.* (12) United States Patent Wang et a]. (45) Date of Patent : (2014).
115. Li, Z. & Wang, C. One-Dimensional nanostructures. 15–29 (2013). doi:10.1007/978-3-642-36427-3
116. Hodgkinson, T., Yuan, X.-F. & Bayat, A. Electrospun silk fibroin fiber diameter influences in vitro dermal fibroblast behavior and promotes healing of ex vivo wound models. *J. Tissue Eng.* **5,** 2041731414551661 (2014).
117. de Moraes, M. A., Nogueira, G. M., Weska, R. F. & Beppu, M. M. Preparation and characterization of insoluble silk fibroin/chitosan blend films. *Polymers (Basel).* **2,** 719–727

(2010).
118. Roylance, D. Mechanical properties of materials. (2008).
119. Ortolani, E. *et al.* Mechanical qualification of collagen membranes used in dentistry. **51,** 229–235 (2015).
120. Suzuki, S. *et al.* Treatment of Silk Fibroin with Poly(ethylene glycol) for the Enhancement of Corneal Epithelial Cell Growth. *J. Funct. Biomater.* **6,** 345–366 (2015).
121. Shadforth, A. *et al.* Incorporation of Human Recombinant Tropoelastin into Silk Fibroin Membranes with the View to Repairing Bruch's Membrane. *J. Funct. Biomater.* **6,** 946–962 (2015).
122. Varanasi, V. ., Shiakolas, P. . & Aswath, P. . Engineering Scaffolds. *Mater. Microstruct. from Nanostructures to Macrostructures Tissue Eng. - Chapter 12* **30,** 3058–3067 (2013).
123. Allardyce, B. J., Rajkhowa, R., Atlas, M. D., Dilley, R. J. & Wang, X. Silk films as a Repair Material for Perforations of the Tympanic Membrane. (2014).
124. Ha, Y. Y., Park, Y. W., Kweon, H. Y., Jo, Y. Y. & Kim, S. G. Comparison of the physical properties and in vivo bioactivities of silkworm-cocoon-derived silk membrane, collagen membrane, and polytetrafluoroethylene membrane for guided bone regeneration. *Macromol. Res.* **22,** 1018–1023 (2014).
125. Wharram, S. E., Zhang, X., Kaplan, D. L. & Mccarthy, S. P. Electrospun Silk Material Systems for Wound Healing. *Macromol. Biosci.* 246–257 (2010). doi:10.1002/mabi.200900274
126. Xu, R. *et al.* Controlled water vapor transmission rate promotes wound-healing via wound re-epithelialization and contraction enhancement. *Nat. Publ. Gr.* 1–12 (2016). doi:10.1038/srep24596
127. Xu, Z., Shi, L., Yang, M., Zhang, H. & Zhu, L. Fabrication of a novel blended membrane with chitosan and silk microfibers for wound healing: characterization, in vitro and in vivo studies. *J. Mater. Chem. B* **3,** 3634–3642 (2015).
128. Tock, R. W. Permeabilities and Water Vapor Transmission Rates for Commercial Polymer Films. 223–231
129. Niemiec, B. A. *Veterinary Periodontology*. (Wiley-Blackwell, 2013). doi:10.1002/9781118705018
130. Primm, J. T. Warning Signs of Periodontal Disease. *The Advanced Institute for Oral Health* (2016). Available at: http://newteethforme.com/signs-of-periodontal-disease/. (Accessed: 3rd June 2016)
131. L. Krese, D. Guided Bone and Tissue Regeneration. *Practice Limited to Periodontics and Implantology* Available at: http://www.davidlkresedds.com/bone-and-tissue-regeneration. (Accessed: 24th August 2016)
132. Murphy, C. M., O'Brien, F. J., Little, D. G. & Schindeler, A. Cell-scaffold interactions in the bone tissue engineering triad. *Eur. Cells Mater.* **26,** 120–132 (2013).
133. Sobajo, C., Behzad, F. & Yuan, X. Silk : A Potential Medium for Tissue Engineering. 438–446 (2008).